ARMY RESEARCH LABORATORY

Using Real-Time Weather Data from an Unmanned Aircraft System to Support the Advanced Research Version of the Weather Research and Forecast Model

by Jeffrey E. Passner, Stephen Kirby, and Terry Jameson

ARL-TR-5950 **April 2012**

NOTICES

Disclaimers

The findings in this report are not to be construed as an official Department of the Army position unless so designated by other authorized documents.

Citation of manufacturer's or trade names does not constitute an official endorsement or approval of the use thereof.

Destroy this report when it is no longer needed. Do not return it to the originator.

Army Research Laboratory
White Sands Missile Range, NM 88002-5501

ARL-TR-5950 **April 2012**

Using Real-Time Weather Data from an Unmanned Aircraft System to Support the Advanced Research Version of the Weather Research and Forecast Model

Jeffrey E. Passner, Stephen Kirby, and Terry Jameson
Computational and Information Sciences Directorate, ARL

REPORT DOCUMENTATION PAGE	Form Approved OMB No. 0704-0188

1. REPORT DATE *(DD-MM-YYYY)*	2. REPORT TYPE	3. DATES COVERED (From - To)
April 2012	Final	July 2010−November 2011

4. TITLE AND SUBTITLE
Using Real-Time Weather Data from an Unmanned Aircraft System to Support the Advanced Research Version of the Weather Research and Forecast Model

5a. CONTRACT NUMBER

5b. GRANT NUMBER

5c. PROGRAM ELEMENT NUMBER

6. AUTHOR(S)
Jeffrey E. Passner, Stephen Kirby, and Terry Jameson

5d. PROJECT NUMBER

5e. TASK NUMBER

5f. WORK UNIT NUMBER

7. PERFORMING ORGANIZATION NAME(S) AND ADDRESS(ES)
U.S. Army Research Laboratory
Battlefield Environment Division
Computational and Information Sciences Directorate (ATTN: RDRL-CIE-M)
White Sands Missile Range, NM 88002-5501

8. PERFORMING ORGANIZATION REPORT NUMBER
ARL-TR-5950

9. SPONSORING/MONITORING AGENCY NAME(S) AND ADDRESS(ES)

10. SPONSOR/MONITOR'S ACRONYM(S)

11. SPONSOR/MONITOR'S REPORT NUMBER(S)

12. DISTRIBUTION/AVAILABILITY STATEMENT
Approved for public release; distribution is unlimited.

13. SUPPLEMENTARY NOTES

14. ABSTRACT
A large information gap exists in available weather data used to initialize mesoscale weather models. Currently, a variety of weather data are used as input for model initialization; however, these data are lacking in remote and dangerous areas in particular and give forecasters a very incomplete overview of the global environment especially in the vertical. For military operations, these data sources may even be more sporadic or inconsistent in time and space due to dangers involved, thus it becomes even more imperative to find alternate sources of model input. One possible solution to this problem is placing meteorological instruments on-board unmanned aircraft systems which would provide observations at a variety of altitudes and time of day when observations are not routinely available. These data can then be input into the Advanced Research version of the Weather Research and Forecasting mode (WRF-ARW). This study explains how this is accomplished and some preliminary results from the flight days.

15. SUBJECT TERMS
Mesoscale, WRF, evaluation, UAS

16. SECURITY CLASSIFICATION OF:			17. LIMITATION OF ABSTRACT	18. NUMBER OF PAGES	19a. NAME OF RESPONSIBLE PERSON
a. REPORT	b. ABSTRACT	c. THIS PAGE			Jeff Passner
Unclassified	Unclassified	Unclassified	UU	70	19b. TELEPHONE NUMBER (*Include area code*) (575) 678-3193

Standard Form 298 (Rev. 8/98)
Prescribed by ANSI Std. Z39.18

Contents

List of Figures

List of Tables

Acknowledgments

The authors would like to extend special thanks to U.S. Army Research Laboratory (ARL) meteorologists David Sauter, John Raby, Robert Dumais, Robert Brown, and Yasmina Raby for their contributions to this project. Additional thanks to Peter Childs of AirDat, LLC for his help with data formatting issues.

INTENTIONALLY LEFT BLANK.

Executive Summary

Problem

An information gap exists in available weather data used to initialize mesoscale weather models, particularly for tactical environments and in the lower planetary boundary layer. Currently, an assortment of both direct and indirect sources of weather data are utilized as input for numerical weather model initialization; however, data are often considerably sparser in remote areas resulting in an incomplete overview of the atmosphere especially in the vertical. For military operations, the data sources may even be more sporadic in time and space due to the dangers involved in their collection and because of severe communication bandwidth constraints; thus, it becomes more crucial to find alternate sources of input for the model. One possible solution to this problem is placing meteorological instruments on-board unmanned aircraft systems, which would provide observations at a variety of altitudes and time of day when they are not otherwise available. These data can then be incorporated into a numerical weather prediction model, such as the Advanced Research version of the Weather Research and Forecasting model (WRF-ARW) through the use of atmospheric data assimilation methods.

Results

To improve the input data sources, The U.S. Army Research Laboratory (ARL) combined with the Physical Sciences Laboratory Technical Analysis and Applications Center and AirDat to design a system where the Tropospheric Airborne Meteorological Data Reporting (TAMDAR) system was developed to fly on an Unmanned Aerial System (UAS) called a TAMDAR-U. Data collected by the TAMDAR-U were then ingested into the WRF model using Four-dimensional Data Assimilation (FDDA). Four flight days were conducted, three of which were discussed in detail in this report. Afterwards, for each test day a double-nested configuration of WRF was run centered near the test site location.

It was found in this study that the "method" works. ARL was able to gather data using TAMDAR-U instruments on an UAS and then assimilate these data into the WRF. This can be a very useful tool for the Army in data-sparse regions. The UAS is robust enough that it can fly at many levels and can fly for extended periods of time to provide continuous assimilation into the model. The fact that it can produce high frequency and multilevel direct observations of critical weather parameters (temperature, humidity, winds) was very advantageous for the FDDA observation nudging strategy used in this study.

Comparing the model output with and without the FDDA data, it was found that the temperature fields do not show much change between model runs, although this has not been verified with any statistical methods. It appears that moisture fields show the most variation, while the wind speeds do increase slightly near the UAS location on the grid. The model corrections do

propagate downwind, but these model adjustments can also be seen upwind, far removed from the location of the UAS and where the data were assimilated. Not only do these adjustments occur in space, they also occur in time. Several hours after the flight had ended there were still some slight differences noted in model fields. The model feedbacks were even noted to influence the rainfall amounts hours after the data had been ingested. The changes are seen in all directions and fields, including the vertical. However, as expected the strongest impacts were felt close to the time and space that data assimilation occurred. The results do show the impact of FDDA can influence the model output.

Conclusions

In this work, questions have not been answered about how much of an improvement was made in the model or even if there was improvement. It is uncertain, at this time, if these changes are significant. However, the study did provide an opportunity for ARL scientists to learn the methods need to study FDDA techniques and understand how model output is influenced by these data. The study showed the changes that might be anticipated in the main weather fields and the feedbacks they produce.

Recommendations

Future work by ARL will try and answer these questions with far more data and data sources ingested into the model. Studies will test as to how different variables are influenced, as well as better techniques for nudging coefficients and radii of influence. It is hoped that these studies can provide a much better model solution that can improve weather forecasts in the battlefield at small scales.

1. Introduction

The Battlefield Environment Division of the Computational and Information Sciences Directorate, U.S. Army Research Laboratory (ARL) has an interest in high spatial and temporal resolution weather output with an emphasis on fine-resolution, short-range forecasts. To accomplish this goal, ARL uses the Advanced Research version of the Weather Research and Forecasting model (WRF-ARW). The WRF-ARW (hereafter the WRF) model is a next-generation mesoscale weather prediction system designed to serve both operational forecasting and atmospheric research needs. The WRF features multiple dynamical cores and a software architecture allowing for computational parallelism and system extensibility. The WRF is suitable for a broad spectrum of applications across scales ranging from meters to thousands of kilometers (*1*).

With an Army requirement to run the model at smaller time and space resolutions, the current synoptic and mesoscale networks of surface weather stations, upper-air observations, and Aircraft Communications Addressing and Reporting System (ACARS) observations are often inadequate since they still leave large spatial/temporal gaps. In a military situation, surface observations and upper-air weather balloons are typically even sparser.

In an effort to improve the input data sources, ARL combined with the Physical Sciences Laboratory's Technical Analysis and Application Center (PSL-TAAC) and AirDat LLC to design a system where the small meteorological data instrument called the Tropospheric Airborne Met Data Reporting (TAMDAR) was reengineered to fly on an Unmanned Aircraft System (UAS). This system was called the TAMDAR-U. These data collected by the TAMDAR-U were then ingested into the WRF model using the Four-dimensional Data Assimilation (FDDA) method of observation nudging.

The UAS used in this experiment was the PSL Aerostar. Four flight days were conducted, three during the summer months of 2010 and one during the late autumn season in the vicinity of the Las Cruces International Airport (LRU). Afterwards, for each test day, a double-nested configuration of WRF (version 3.2.1) was run centered near the test site location. The outer nest of 3-km grid spacing was configured with a horizontal dimensionality of 161 × 161, resulting in an areal domain of 480 km × 480 km. The inner nest of 1-km grid spacing applied a horizontal dimensionality of 121 × 121, resulting in an areal domain of 120 km × 120 km. The 12-h forecast period commenced at 1300 Coordinated Universal Time (UTC) using the preceding 0600 UTC North American Mesoscale (NAM) model output as model input. Each test day provided a variety of weather conditions and the on-site ARL meteorologist furnished a pre-flight briefing and worked with the flight crew to present updated meteorological information.

2. The Field Experiment

The PSL-TAAC was established in 1999 with the mission to promote safe integration of UAS in the National Airspace System (NAS). In order for a UAS to be flown in the NAS outside of restricted airspace, a certificate of authorization (COA) or an experimental airworthiness certificate must be issued by the Federal Aviation Administration; COAs have been obtained by New Mexico State University to operate the Aerostar within a large portion of the NAS in southern New Mexico. The PSL-TAAC can provide critical technologies testing, planning for routine flight operations, certification, regulatory, research, and validation and planning for worldwide operations (*2*).

The Aerostar UAS (figure 1) was developed by the Aeronautics Defense Systems in cooperation with the Israeli Intelligence Corps. The Aerostar can perform a variety of missions, and it has a ceiling of about 18,000 ft above mean sea level (MSL) with a possible endurance time of 14 hours. The Aerostar has a line-of-sight data link range of 200 km with a loiter speed of 60 knots and a dash speed of 110 knots. It has a wingspan of 25 ft (7.5 m), a length of 15 ft (4.5 m), a height of 4 ft (1.2 m), a maximum takeoff weight of 460 lb (210 kg), and a maximum payload weight of 110 lb (50 kg). The airframe is powered by a single propeller-driven, two-stroke gasoline engine. Fuel capacity is 15 gal of aviation-grade gasoline. The UAS is fitted with electrical systems consisting of an engine-driven alternator and backup battery. It also features a transponder with Mode C altitude reporting capability, one anti-collision light, and wingtip position lights. The Aerostar has a Controp Precision Technologies Digital Signal Processing (DSP)-1 Electro-Optical/Infra-Red sensor system. The DSP-1 is a high-performance, stabilized dual-sensor system (*3*).

AirDat LLC is a privately-held company formed in 2003 to develop the TAMDAR sensor, implement the supporting infrastructure, and create weather information solutions with the data set. The TAMDAR instrument (figure 2), which weighs only 1.5 lbs, was designed and built by a team led by researchers at The National Aeronautics and Space Administration's Langley Research Center in Hampton, VA. The TAMDAR system comprises a patented multi-function atmospheric sensor installed on commercial scheduled aircraft, a near-real-time satellite data communication system (the Iridum satellite constellation), and AirDat's ground-based data processing and distribution systems. The intention of TAMDAR observations is to fill in the gaps in conventional atmospheric data to hopefully create more accurate high resolution weather forecasts. The TAMDAR sensor is a lightweight, low drag (0.4 lb at 200 knots), low power device designed for easy installation and retrofit to any aircraft. It is a stand-alone system that does not require interaction with any critical aircraft systems; this simplifies certification and crew training requirements. TAMDAR has been installed on a wide range of airframe types, although twin- or multi-engine aircraft offer the broadest choice of mounting locations. AirDat

currently has over 150 TAMDAR airborne sensors installed in commercial airliners flying daily into airports throughout North America including Alaska and Mexico (*4*).

Figure 1. A photo of the Aerostar UAS.

Note: The source for figure 1 is the Aeronautics Defense Systems website (*5*).

Observations are taken at specified pressure altitude levels (remotely programmable by AirDat) as the aircraft takes off and climbs to cruise altitude. At cruise level, observations are switched to a time-based protocol (also remotely programmable) and then switched back to pressure-based levels as the aircraft descends to land. As they are made, observations are transmitted to AirDat's data center and are typically available for model assimilation or analysis within a minute of the time of observation. AirDat employs a two-way satellite communication system to downlink TAMDAR data and uplink sensor commands. The data center receives, processes, quality controls, archives, and distributes TAMDAR atmospheric data in effectively real-time and can provide other data link, modeling, and analysis solutions, as well as network services to weather information customers and aircraft operators. Atmospheric measurements performed by the TAMDAR sensor include:

- Humidity
- Pressure altitude and static pressure
- Air temperature

- Winds aloft
- Icing
- Turbulence
- Location, time, and altitude from built-in GPS

Figure 2. The TAMDAR instrument on commercial aircraft weighs only 1.5 lbs.

Note: The source for figure 2 is the National Aeronautics and Space Administration (NASA) TAMDAR website (*6*).

Part of the purpose of the field exercise and project described herein was to demonstrate that a meteorological sensing system could be sufficiently downsized in terms of its weight, physical size, and power consumption and that it could be successfully operated on a relatively small aircraft, such as the Aerostar. AirDat redesigned the TAMDAR sensor so that it would be smaller and lighter on the Aerostar. A reduction in the size of the probe size, box size, system weight, and power consumption reduced the weight of the TAMDAR (herein called TAMDAR-U) from 32 oz to 14.4 oz. Additionally, it became necessary to mount the TAMDAR-U sensor probe on the nose cone of the UAS due to a lack of the required structural strength of the Aerostar's fuselage, as well as disruptions of the proper airflow around the body of the aircraft. These changes are displayed in figures 3 and 4.

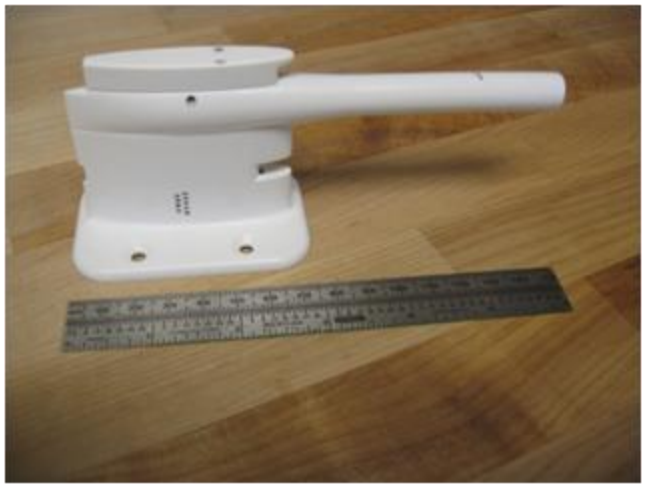

Figure 3. Prototype TAMDAR-U sensor probe.

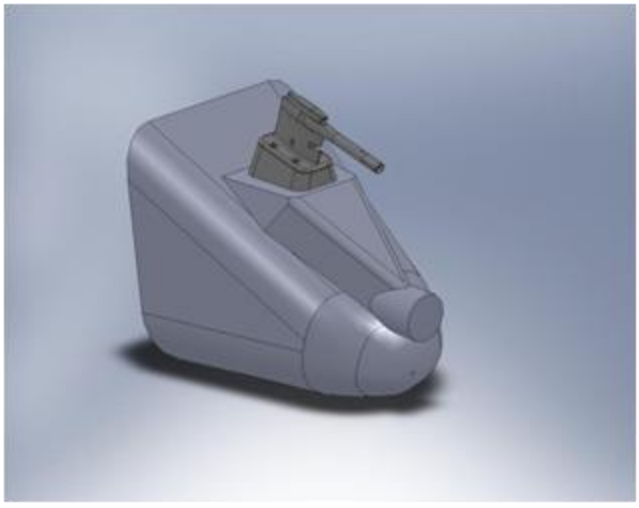

Figure 4. Artist rendering of sensor probe as mounted on the modified Aerostar nose cone.

Until this point, UAS generated readings were only viewable by their pilots and could not be disseminated to other users or for ingest into weather forecast models. The meteorological sensors on UAS also have had no mechanism in place to conduct quality control checks on the data they produce.

The TAMDAR system, on the other hand, transmits its data to a satellite network from anywhere in the world, and the meteorological observations are transmitted to a ground station where extensive quality checks are run. Subsequently, the data are properly reformatted so that they can be ingested into weather forecast models.

ARL was responsible to organize and conduct the tests of the instrument. As such, ARL researchers developed the flight test profiles to optimize the data collection opportunities, designed the data analysis methodology, and conducted the evaluation of the datasets that were

collected. PSL and AirDat collaborated to conduct initial flights to test instrument calibration as required by AirDat, to ensure the instrument was producing accurate positioning and heading readings.

A number of obstacles were encountered during the course of the TAMDAR-U project, not only from the standpoint of the proper collection of meteorological data, but also in the engineering design phase as the instrument was being installed on the Aerostar UAS.

It became obvious that the placement of the TAMDAR-U instrument in the Aerostar's payload bay was going to be a critical and difficult issue. The Aerostar can carry a payload of up to approximately 110 lbs (50 kg); however, due to the aircraft's small overall weight and size, its balance can easily be disrupted if the payload is not very precisely situated. Although the TAMDAR-U is light-weight, it still had to be centered on the longitudinal axis of the aircraft to maintain proper balance and flight characteristics. This requirement was not difficult to achieve, however, it introduced a new complication. The TAMDAR units deployed on the commercial airliner fleet have the sensor probe mounted directly on the data acquisition unit itself. A hole is drilled in the fuselage through which the probe extends. The TAMDAR is then bolted onto the inside of the fuselage. For TAMDAR-U, the probe had to be redesigned, detached from the instrument case, and connected to it by a short cable segment. The sensor probe was then mounted on the top of the Aerostar's nose cone.

Another issue was exactly how to mount the sensor probe. The airflow along the fuselages of commercial airliners is fairly uniform and there is greater flexibility concerning where the TAMDAR probe can be mounted. In this case, the mounting plate on the nose cone had to be precisely offset from horizontal (by about 11°) so that the impinging wind stream would directly enter the probe tube while the aircraft was in a level flight configuration, and correct sampling would be achieved.

In order for TAMDAR-U to determine the wind direction and speed, the aircraft's precise heading must be known. AirDat's engineers had assumed that the TAMDAR-U could draw heading information from the Aerostar's on-board data bus (which had heading data available). Due to proprietary restrictions imposed by the aircraft's manufacturer, this connection was not approved. As a result, a separate heading instrument knows as a magnetometer had to be procured. Although the magnetometer is a small instrument with limited power draw, its installation added a minor complication that had not been foreseen originally.

Along with the various engineering problems that had to be resolved, the TAMDAR-U project involved a number of data collection issues as well. It became apparent that the optimum meteorological data collection scenarios envisioned by ARL were almost diametrically opposed to the PSL-TAAC mission commander's (MC) most desirable flight operations. Ideally, TAMDAR-U data should have been collected in the lower boundary layer (around 300 m above ground level [AGL] and below) and at ranges up to 80 km from the model center point (which was close to the Las Cruces airport), toward the far southwestern and northwestern corners of the

domain (over the most varied terrain). Furthermore, it would have been preferable to collect data during episodes of marginal or adverse weather (strong winds, low visibility, in or near clouds and/or precipitation, etc.). In this way, the potential for accuracy improvement of the WRF system (with ingest of the high-resolution TAMDAR-U data) would have been maximized. As it turned out, the opposite was the case. The MC preferred to fly in the most benign weather conditions possible (light winds, clear skies, and good visibility). Also, due to terrain interference and flight control system issues, the uplink from the ground station to the Aerostar would lose integrity at times, especially while flying at lower altitudes AGL and at greater ranges from the airport. As a result, in most cases the data collection patterns were closer to the airport (within about 30 km) and at higher altitudes, typically above 1000 m AGL.

The COA mandates that a "chase plane" must accompany the Aerostar when it is flown beyond the immediate airport traffic pattern, and its crew must maintain visual contact with the UAS at all times. This COA condition meant that the aircraft could not be flown before sunrise or after sunset, and for the sake of the chase plane crew, data collection missions were restricted to approximately 3 hrs duration.

The team conducted data collection flights on four occasions during which full observation datasets was obtained on the dates and times listed in table 1.

Table 1. Aerostar flight times during the four testing periods.

Date	Start Time (UTC)	End Time (UTC)
15 July 2010	1435	1743
16 July 2010	1429	1751
20 Aug. 2010	1538	1720
2 Dec. 2010	1525	1841

3. The WRF and Four-Dimensional Data Assimilation

The WRF used in this study was WRF version 3.2.1. To resolve the local terrain features, a double-nested configuration was adopted for the model. The nests were centered near the test site location, at 33.22° N and 107.17° W, as shown in figure 5, which shows the inner domain, Domain 2. The outer 3-km domain was 161 × 161 in horizontal dimensionality and inner 1-km grid was 121 × 121 grid points. The model had 90 terrain-following vertical levels.

The 12-h forecast period commenced at 1300 UTC (typically the hour before the flights began) and ran until 0100 UTC the next day in an effort to include the late-afternoon local Santa Teresa, NM sounding as a possible verification source. The 0600 UTC NAM data was used to initialize the lateral boundary conditions. A summary of the WRF-ARW model physics used by ARL is listed below:

- Thompson Microphysics
- No cumulus parameterization scheme
- 3:1 grid space (km) to advected time step ratio
- Dudhia short-wave radiation
- Rapid Radiative Transfer Model (RRTM) long-wave radiation
- Noah Land Surface model
- Quasi-Normal Scale Elimination Planetary Boundary Layer and surface layer schemes
- Terrain slope/shadow option used

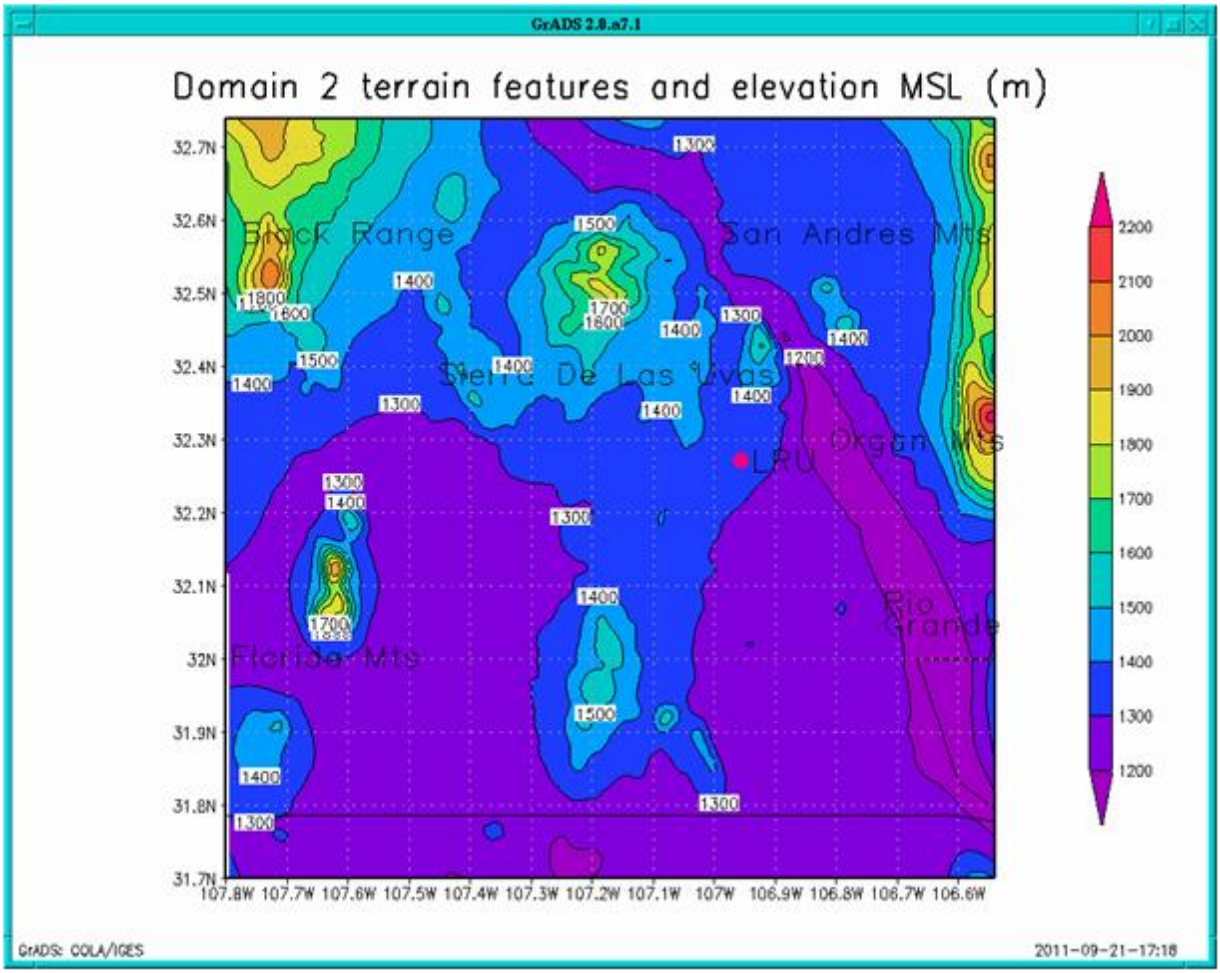

Figure 5. Shaded terrain and contours (m) for the 1-km grid centered near the Las Cruces, NM airport.

The inner grid contained a variety of terrain features as shown in figure 5. LRU is displayed by the red dot. Mountain ranges on the east border of the domain are known as the Organ Mountains

and the San Andres Mountains. To the southwest are the Florida Mountains, while the higher Black Range lies in the northwest corner of the domain. Just northwest of LRU is the Sierra De Las Uvas range, which is where the Aerostar tests on July 15 and July 16 were centered. In the east central region of the domain, the Rio Grande River and Rio Grande valley are captured by the lowest contoured elevation region running NW-to-SE.

FDDA is a form of continuous atmospheric data assimilation, where forecast values of temperature, wind, and moisture are nudged toward the ingested observations through the use of additional relaxation or artificial "forcing" terms in an effort to improve forecast quality and performance. This is a particularly powerful tool in data-void regions where surface and upper-air data are typically not dense or regularly available. However, it is also useful in data-rich areas as well (*7*).

In this study, the critical user-defined weighting parameters used in determining the strength and extent of observation nudging at model grid points was based upon past experience at ARL and suggestions provided by National Center of Atmospheric Research (NCAR) modelers. The weighting parameters involve defining for observations a radius of influence in both the horizontal and vertical, a nudging time window, and a nudging/relaxation strength coefficient. All of these parameters and weights are set in the WRF model's "namelist" or input file.

In observation nudging, the difference between the model state and observed state is computed at the observation locations, and analyzed back to the grid in a region surrounding the observations (*8*). At a given time step and grid point (x,t), the tendency term added to the equations is proportional to

$$G_{\alpha} \cdot \sum_{i=1}^{N} W_i^2 \ (x,t)\gamma_i(\alpha_{ob} - \alpha)_i \Big/ \sum_{i=1}^{N} W_i \ (x,t) \tag{1}$$

where the summation is over all the observations within a radius of influence from the given grid point. The observation quality factor, γ, ranges from 0 to 1 (although not used in this version of WRF).

The nudging coefficient Gα determines the magnitude of the nudging term. A relatively large nudging term should be used to nudge high-frequency data while the nudging term should be small compared to the total tendency term in the prognostic equation. Typical values are close to the magnitude of the coriolis term forcing, in our case 1.0×10^{-3} s^{-1}. The goal is to allow the model fields to adjust towards the observations without overfitting to the individual observations.

The weighting for observation *i* is determined by the spatial and temporal separation of the observation and grid point and can be written as

$$W(x,t) = w_{xy} \cdot w_z \cdot w_t \tag{2}$$

Currently, the horizontal weighting function is a Cressman-type function as shown in equation 3.

$$w_{xy} = \frac{R^2 - D^2}{R^2 + D^2} \quad (3)$$

The vertical weighting function and the temporal weighting function are also "distance" weighted in a similar fashion. The values of the nudging parameters are determined by the user as are the radius of influence and time window around the observation time. The values used for FDDA in this study are listed below:

- FDAA ran for approximately 4 hrs; between 1300−1700 UTC for all cases
- Wind, temperature, and moisture are nudged
- Nudging coefficient G = 1×10^{-3}
- Radius of influence Domain 1 = 20 km, Domain 2 = 10 km
- Radius of influence vertically 0.1 sigma
- Window for observation input 45 min
- Ramp down time 40 min

4. Case Study 1: 15 July 2010

A large ridge of high heights aloft dominated the southwest United States on this day; thus, presenting subsidence and tranquil flying conditions for the Aerostar as seen in the satellite photo in figure 6.

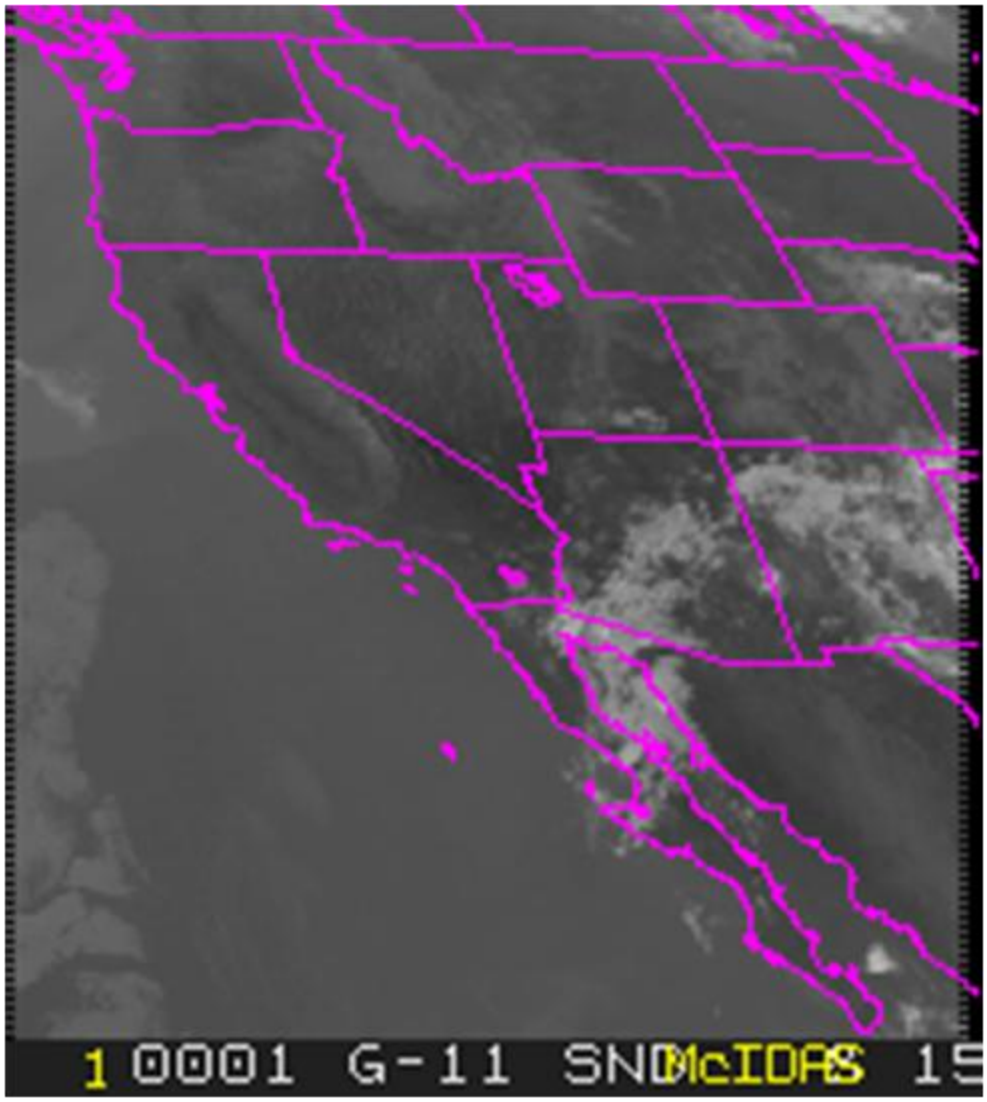

Figure 6. Multi-functional Transport satellite image over western United States valid at 1500 UTC 15 July 2010.

Note: The source for figure 6 is (http://dcdbs.ssec.wisc.edu) (*9*).

The 1200 UTC upper-air sounding (figure 7) from Santa Teresa displayed warm temperatures with light and variable winds through much of the atmospheric column. A layer of slightly enhanced winds was noted from 850 hPa to 780 hPa where westerly to northwesterly winds from 10 to 14 knots were observed. Otherwise, winds were less than 10 knots through the middle atmosphere. There was a layer of higher relative humidity observed in the sounding, which is supported by higher-level (550 to 400 hPa) cloud cover on the satellite image in figure 6.

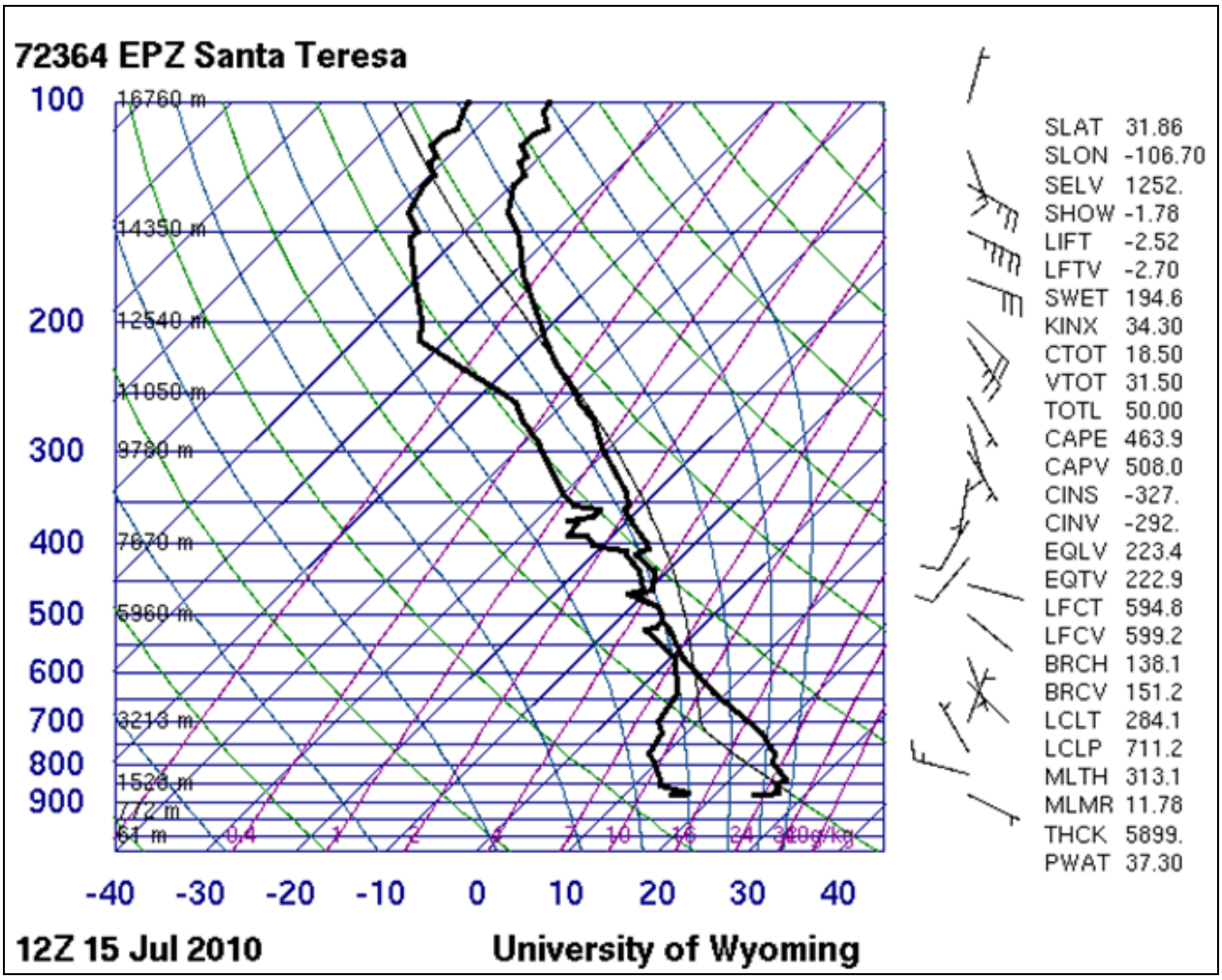

Figure 7. Upper-air observation at 1200 UTC 15 July 2010 from Santa Teresa, NM.

Note: The source for figure 7 is the University of Wyoming, Department of Atmospheric Sciences website (*10*).

One of the goals on this day was to investigate the influence of the ingested data at flight level and see how high and low above the flight level these data affected the model output. The wind data at flight level is seen in figures 8 −10, where figure 8 shows the winds with no TAMDAR data, figure 9 displays the winds with TAMDAR data, and figure 10 gives a three-dimensional look of the wind speeds over the grid.

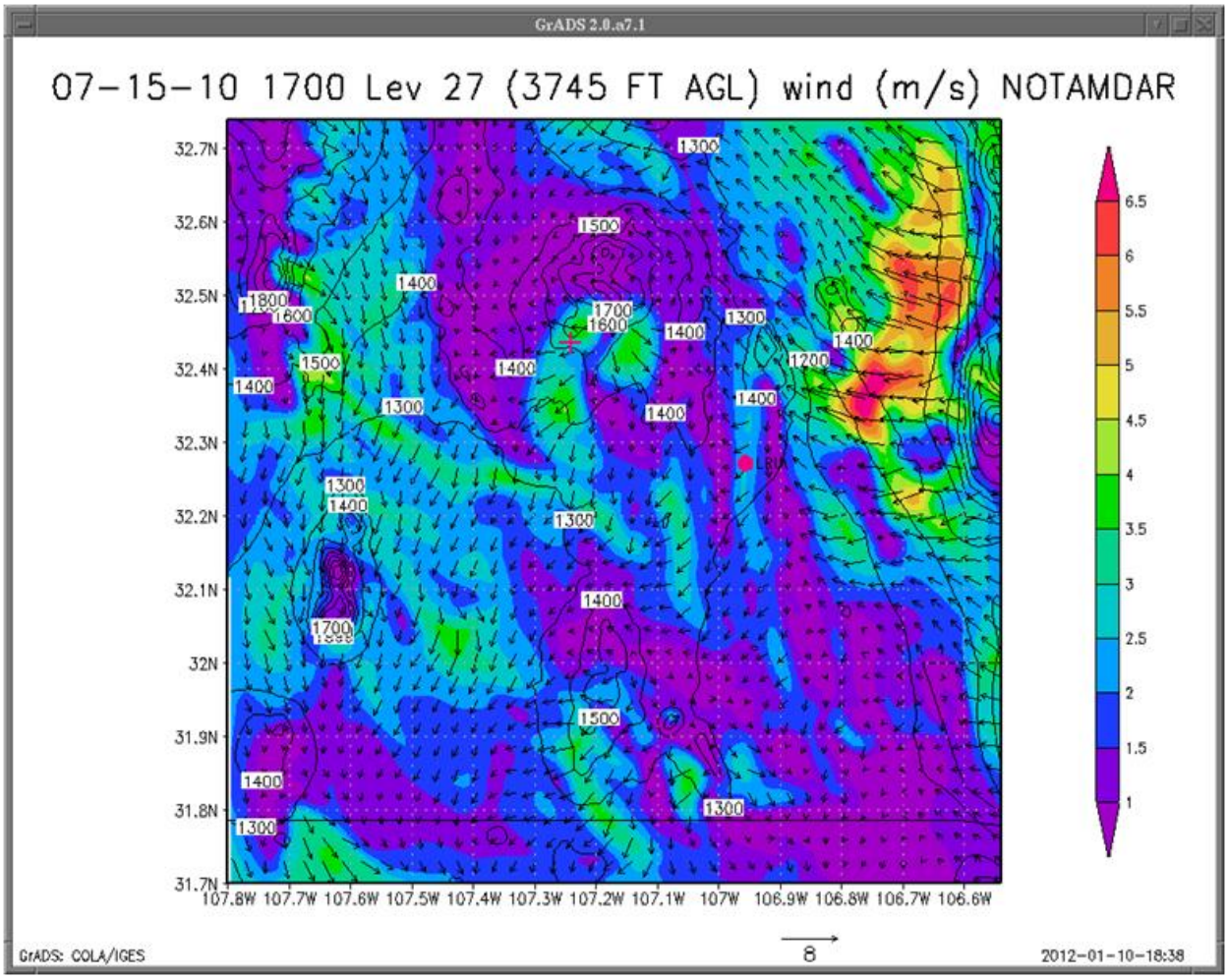

Figure 8. 15 July 2011 1700 UTC WRF wind speed and wind direction forecast at flight level (3745 ft AGL) without ingesting TAMDAR-U data.

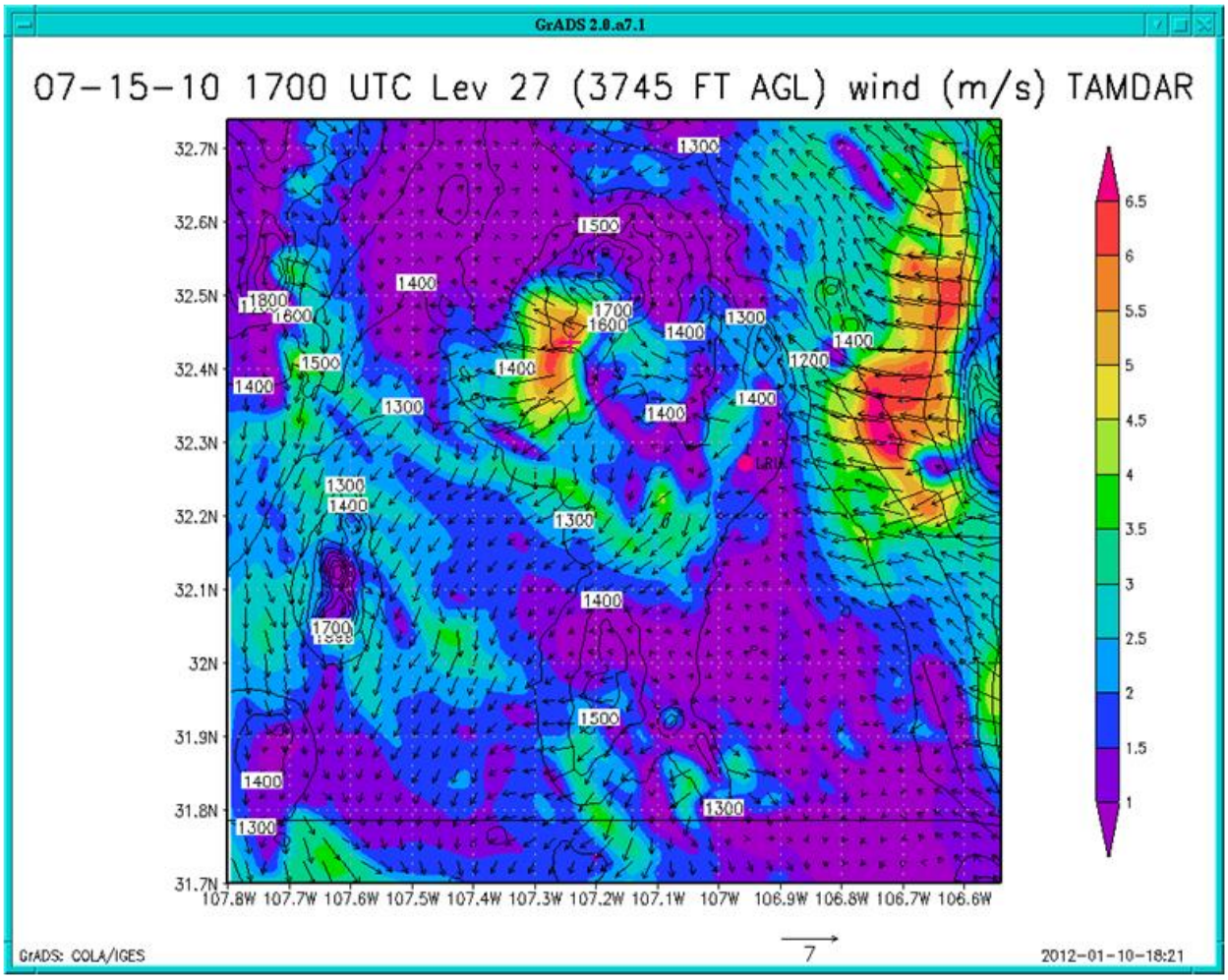

Figure 9. 15 July 2011 1700 UTC WRF wind speed and wind direction forecast at flight level (3745 ft AGL) with TAMDAR-U data ingested.

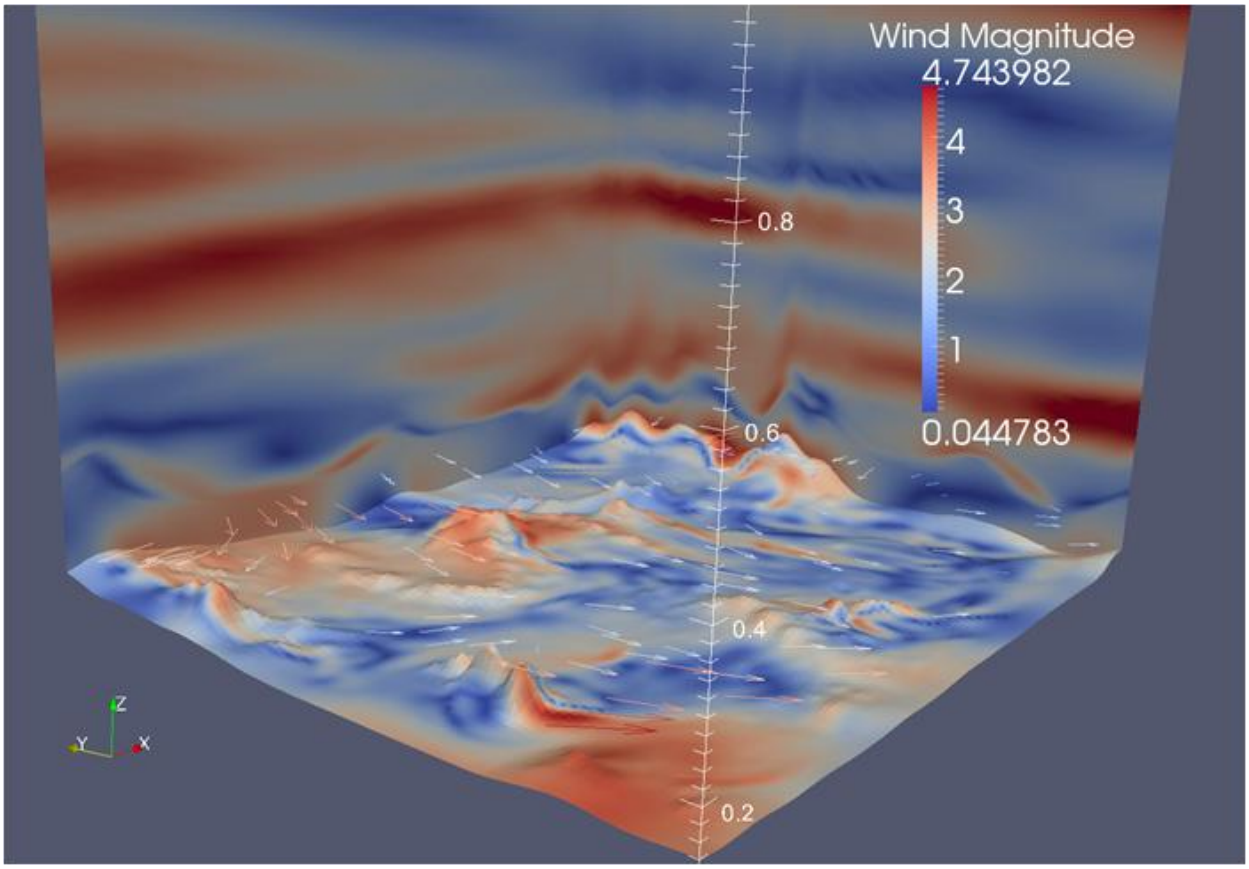

Figure 10. Three-dimensional display (using Paraview V3.0) with ingested FDDA data of Domain 2 wind speeds at 1700 15 July 2010 with the flight level wind barbs colored using the wind speeds shown in wind magnitude bar. Units of height are km/10. Wind speeds are in m/s.

The flight level on 15 July averaged 3745 ft AGL at around 1700 UTC with a path from the Las Cruces airport to the northwest over the Sierra de Las Uvas Mountains. The Aerostar flew over and near the mountain range through much of the flight. The Aerostar location is marked by the red crosshair starting with figure 8 while LRU is marked by the red dot.

There are differences noted on the plots with and without the TAMDAR-U data. Figure 8 shows the wind speed and wind direction without ingesting the TAMDAR-U data while figure 9 displays the wind output with TAMDAR-U flight level data included. The strongest winds in figure 9 are noted on the downslope or west side of the San Andres Mountains on the east edge of the grid. There does not seem to be much difference in the wind speeds and directions between figure 8 and figure 9; however, that is not the case near the Sierra de Las Uvas in the north central part of the domain. Near the Aerostar location, there is an obvious enhancement of wind speed and a stronger westerly component of the flow at the flight level as seen in figure 9. A three-dimensional view of the domain is shown in figure 10, which displays the wind speeds (m/s) and wind barbs over the terrain.

The next set of figures shows the relative humidity (RH) fields at level 27. Figure 11 displays the RH forecast without the TAMDAR while figure 12 shows the RH forecast with the TAMDAR data included. Both figures also include the forecasted wind fields.

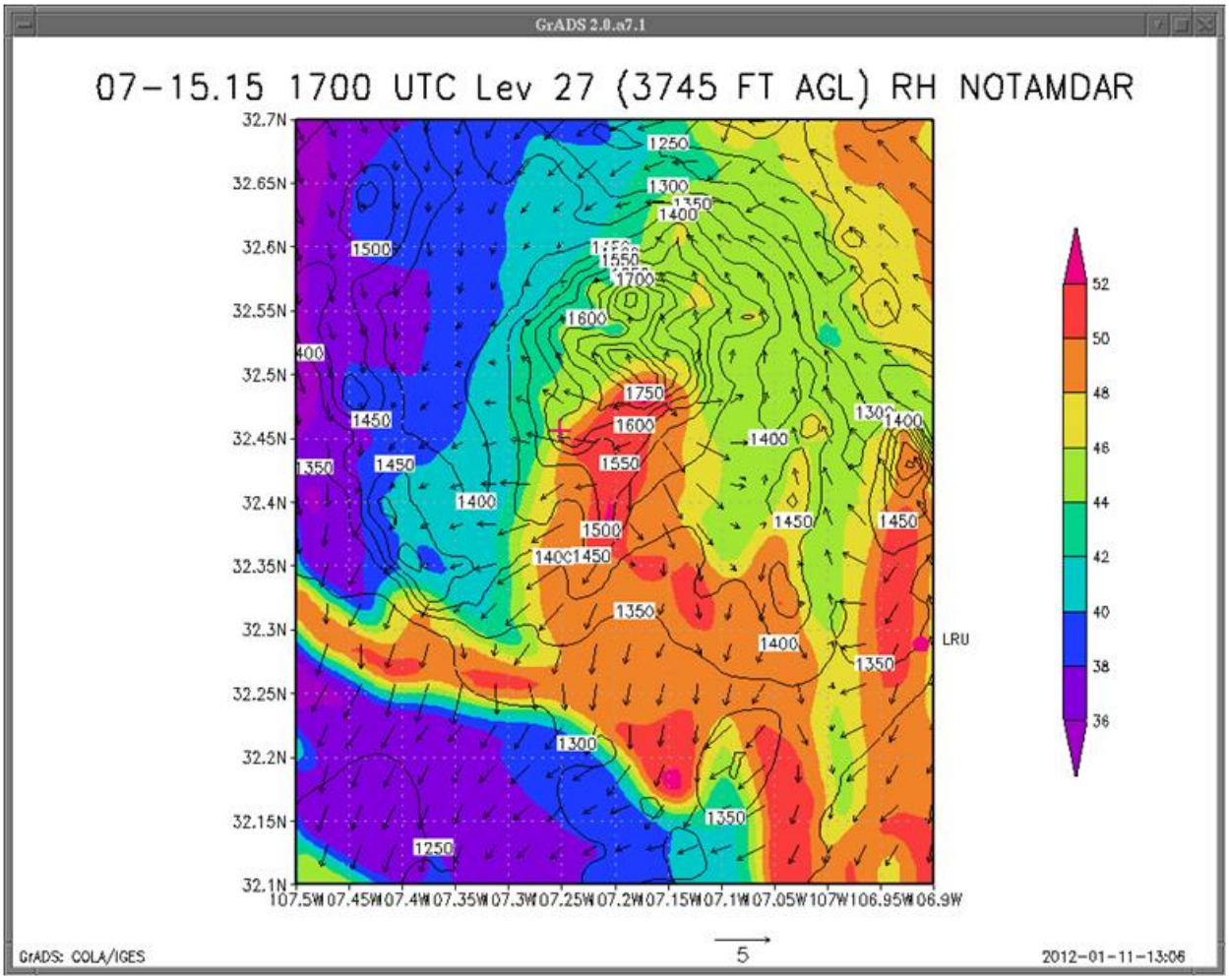

Figure 11. 15 July 2011 1700 UTC WRF wind speed and RH forecast at Level 27 (3745 ft AGL) with no TAMDAR-U data.

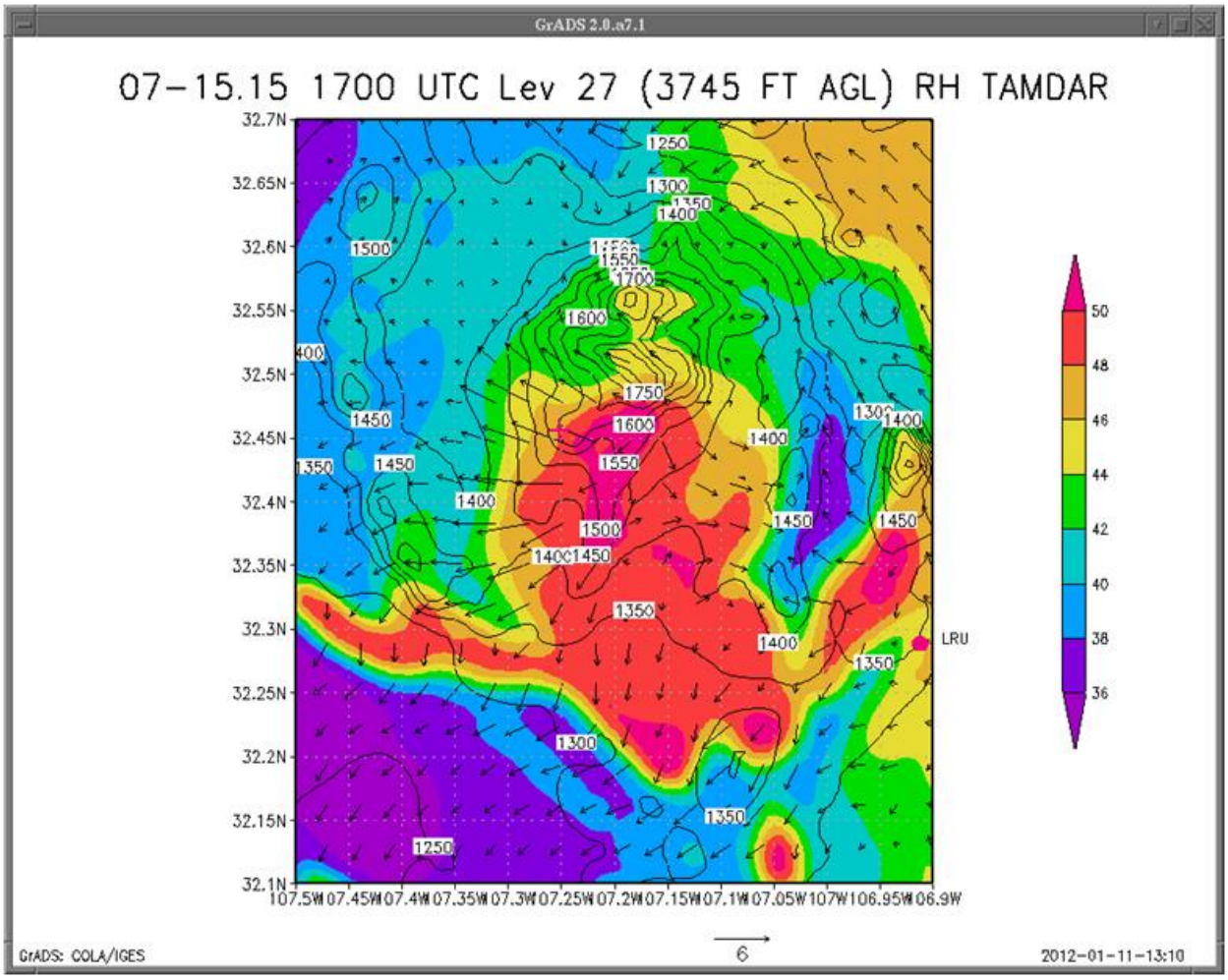

Figure 12. 15 July 2011 1700 UTC WRF wind speed and RH forecast at Level 27 (3745 ft AGL) with TAMDAR-U data.

As seen in figure 11, the highest RH is just to the south of the Sierra de Las Uvas. There are not significant differences noted in the RH patterns, although there is a distinct area of lower RH to the east of the mountains in figure 12. Plots of the vertical motion fields (not shown) indicate similar trends with light rising vertical motions below flight level and weak sinking motions above the flight level to the east of the mountains. However, the vertical motion fields near the mountains are higher with the TAMDAR data. Thus, it can be concluded that the vertical motion fields and any sinking and rising motion have not influenced the RH fields east of the mountains. At 1700 UTC, the dew point at Level 27 with the FDDA completed is 5.7 °C while the case without FDDA is 7.7 °C. This 2 °C difference in dew point is the cause of the lower RH values. The TAMDAR-U data shows RH values on average of 40% near 1700 UTC. Additionally, the inclusion of the TAMDAR-U wind data adds a more northwesterly component to the wind direction, which advects this drier area to the location noted in figure 12.

To see the wind speeds and wind direction with more clarity, figures 13 and 14 show the wind closer to the center of the grid. Figure 13 shows the wind data without TAMDAR-U input while figure 14 displays the data with the TAMDAR-U data. There is a more concise area of stronger winds in the vicinity of the UAS to the southwest of the Sierra de Las Uvas. Meanwhile, there are weaker winds to the northeast of the mountains with the TAMDAR-U data being assimilated.

One of the goals on this day was to show the different responses in the temperature, wind, and moisture fields with the addition of the TAMDAR-U data. These variations are seen in many cases at the flight level, but also on levels above and below the flight level. At Level 16, 2654 ft AGL, there are slightly different winds in the central and northern part of the grid as observed in figure 15 and figure 16. Additionally, there are differences noted at Level 32, 4939 ft AGL, as shown in figure 17 and figure 18. In figure 17, the case without the TAMDAR-U data, the winds are generally light and variable above the valley floor, however; in figure 18, with TAMDAR-U data included, the WRF model output shows lighter winds above LRU but stronger winds near the UAV location. As noted above, these variations are probably associated with the model's vertical and horizontal advection of the TAMDAR-U data ingested.

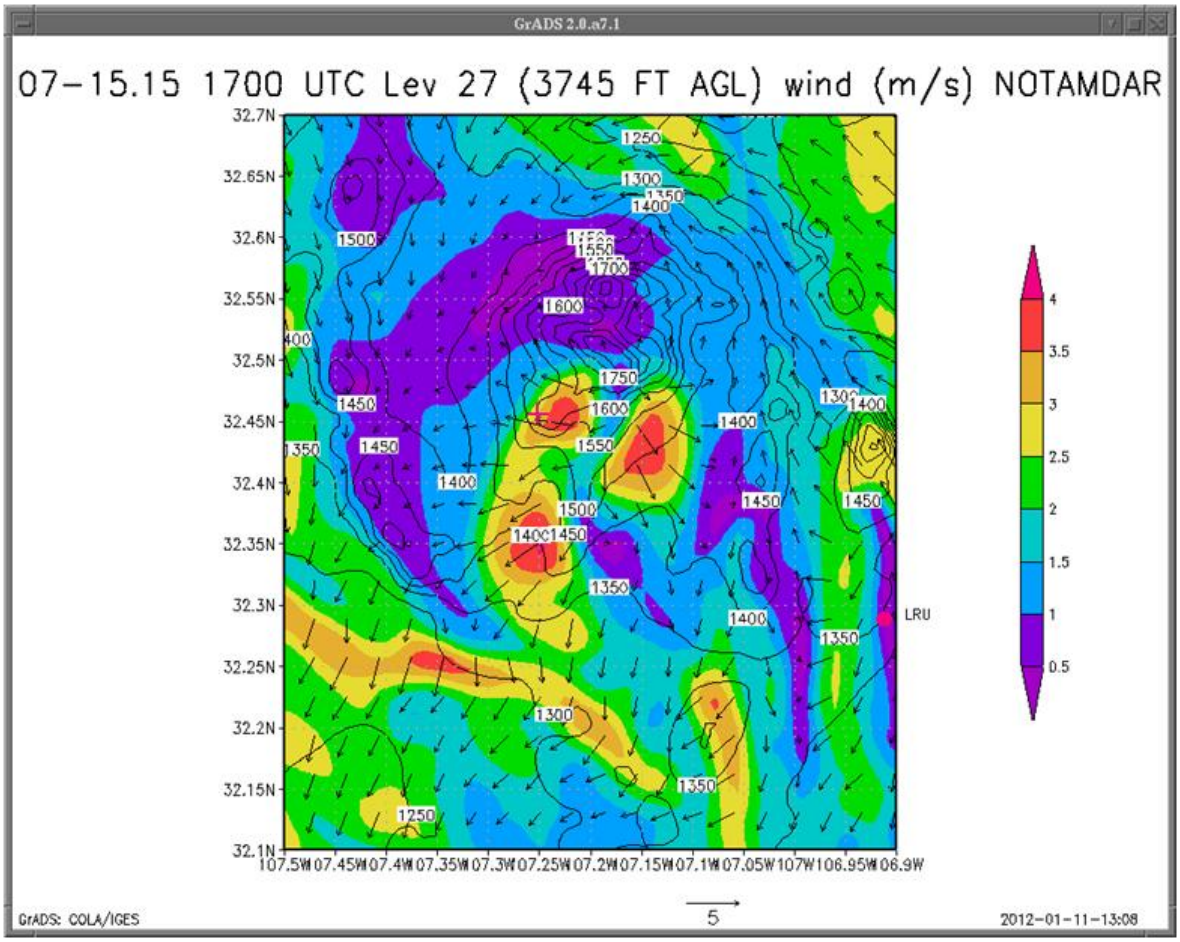

Figure 13. 15 July 2011 1700 UTC WRF wind speed and wind direction forecast at Level 27 (3745 ft AGL) with no TAMDAR-U data.

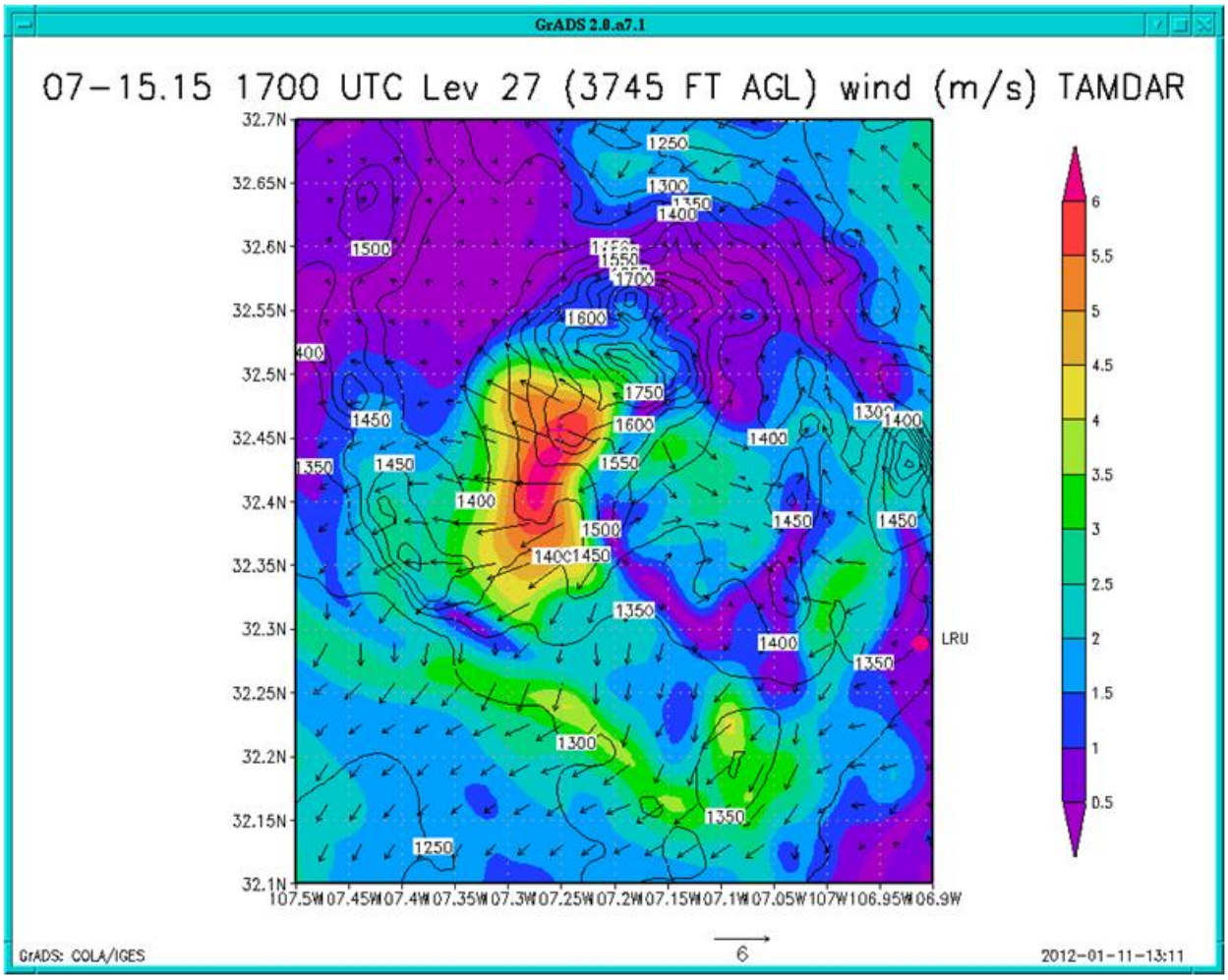

Figure 14. 15 July 2011 1700 UTC WRF wind speed and wind direction forecast at Level 27 (3745 ft AGL) with TAMDAR-U data.

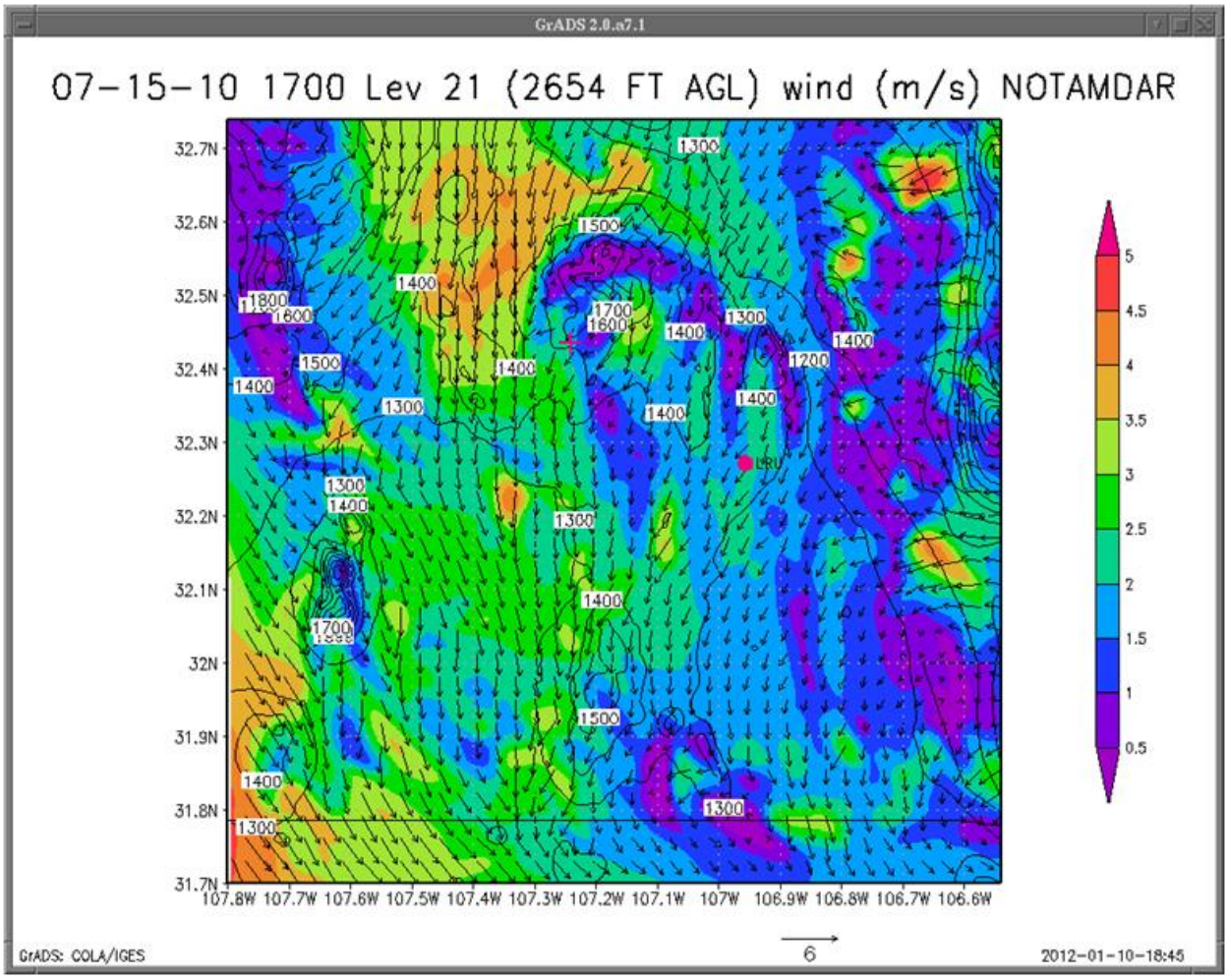

Figure 15. 15 July 2011 1700 UTC WRF wind speed and wind direction forecast at Level 21 (2654 ft AGL) with no TAMDAR-U data.

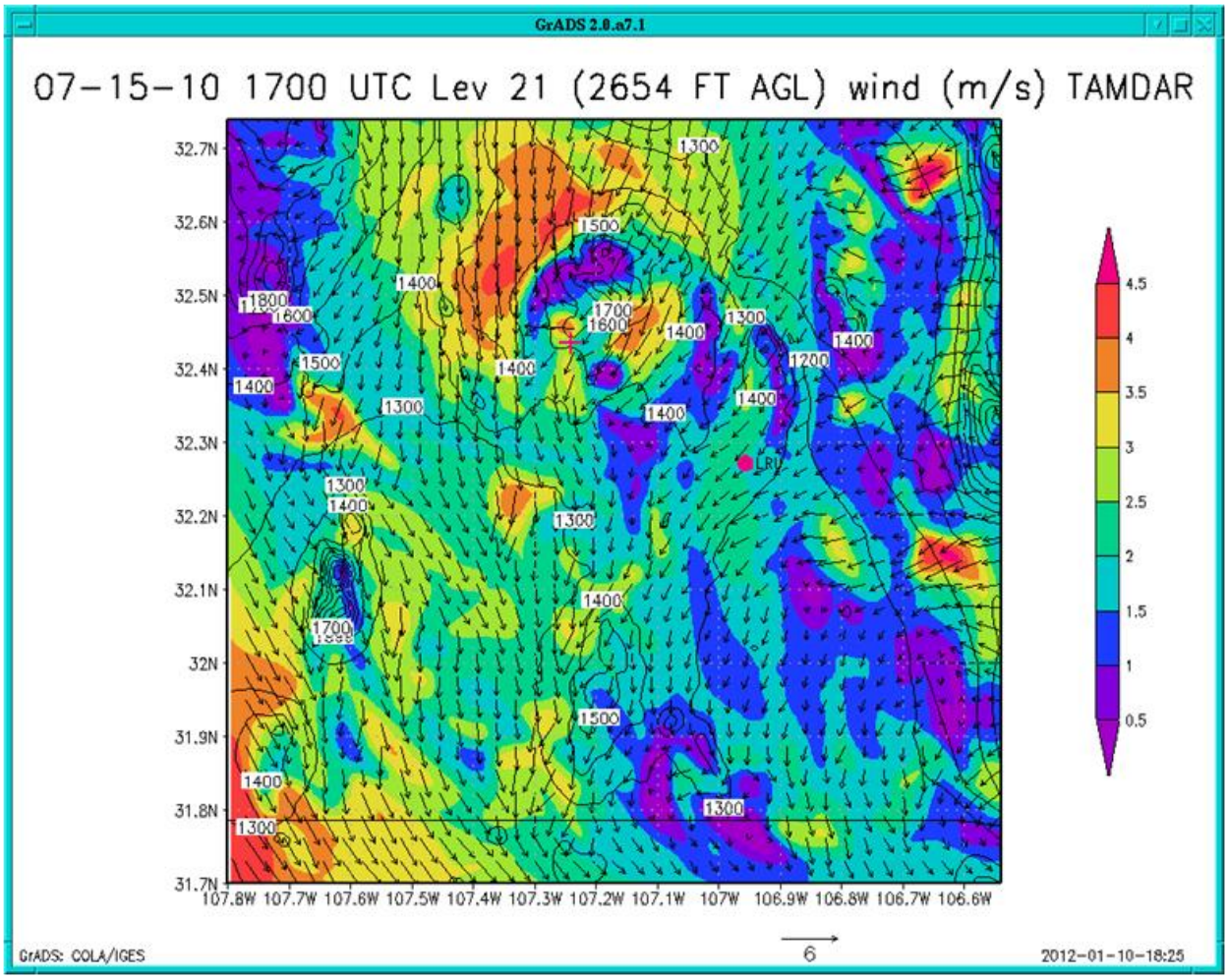

Figure 16. 15 July 2011 1700 UTC WRF wind speed and wind direction forecast at Level 21 (2654 ft AGL) with ingested TAMDAR-U data.

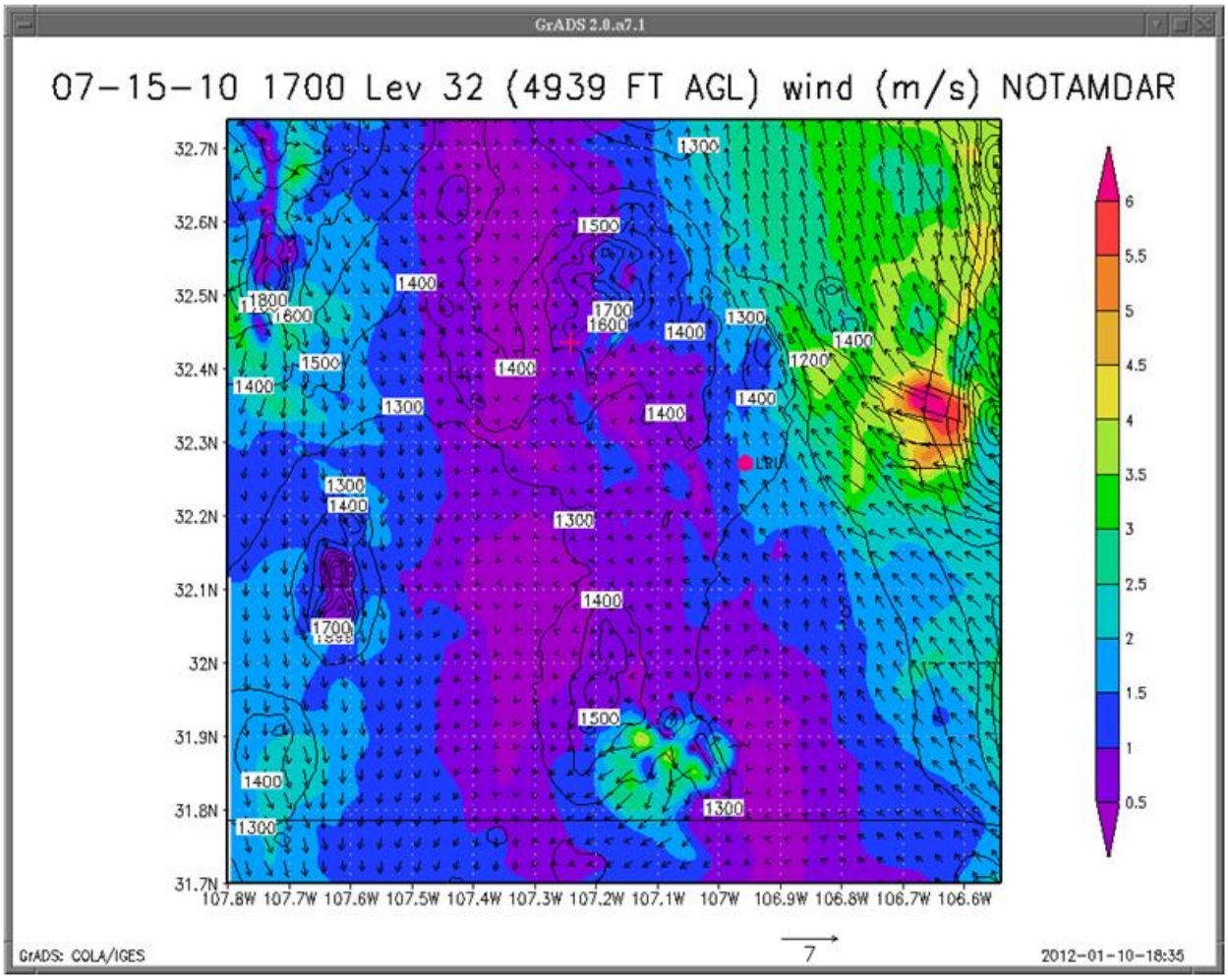

Figure 17. 15 July 2011 1700 UTC WRF wind speed and wind direction forecast at Level 32 (4939 ft AGL) with no TAMDAR data.

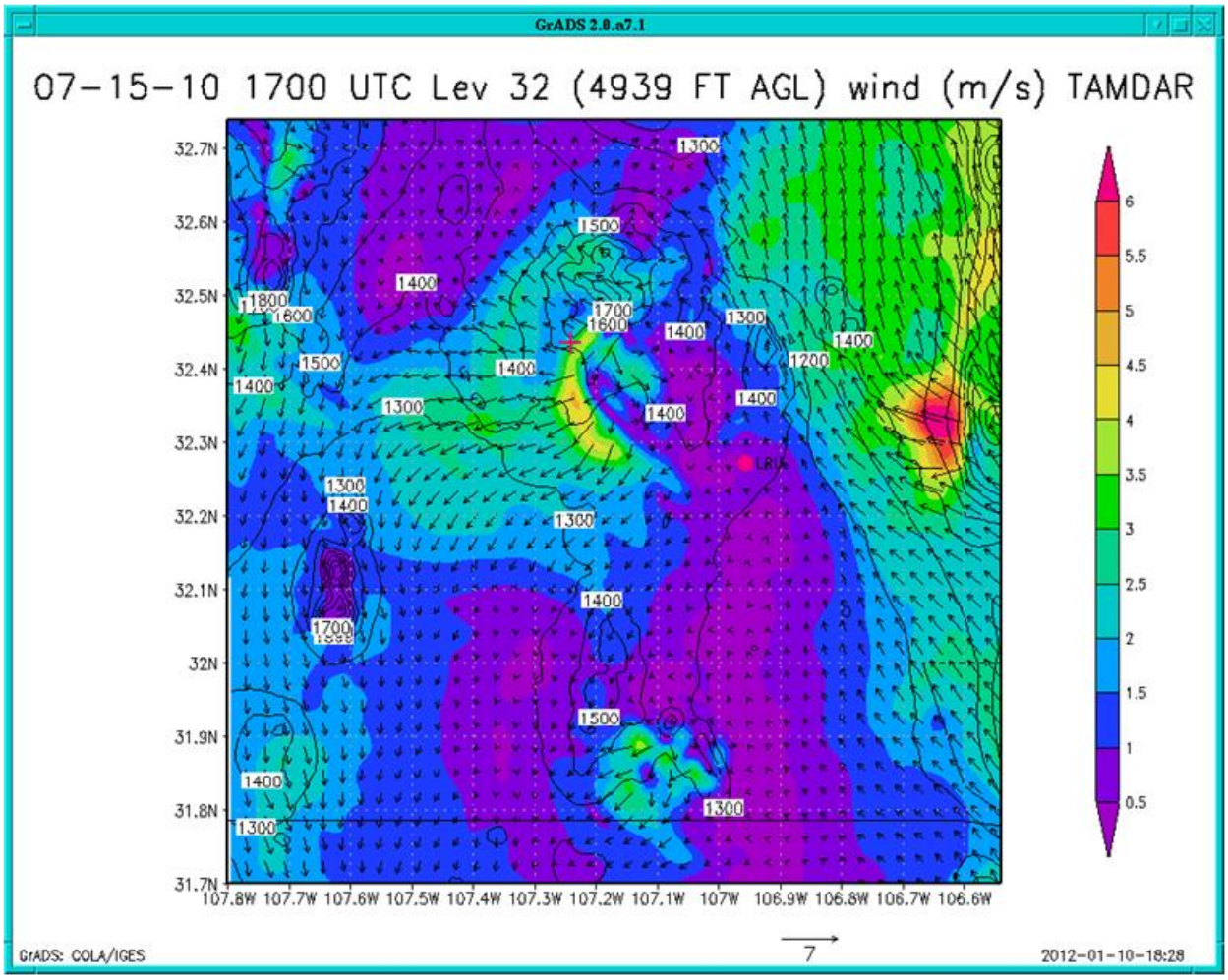

Figure 18. 15 July 2011 1700 UTC WRF wind speed and wind direction forecast at Level 32 (4939 ft AGL) with TAMDAR-U data.

While not shown here, the surface winds with TAMDAR-U data and surface winds without the TAMDAR-U data showed no significant differences. This might be expected since no surface data was ingested. Only the data at the flight level was used, but there are still influences above and below the flight level. It is uncertain to what height above and below the flight data the TAMDAR-U data influences the model solution; however, there are differences noted at 1,000 ft and 2,000 ft above and below the flight level with apparently less influence vertically from the flight level.

5. Case Study 2: 16 July 2010

The flight began at LRU at 1428 UTC and ended at about 1730 UTC on a day with broken high overcast skies as can be seen in figure 19, a satellite photo about midway through the Aerostar flight. The 1200 UTC upper-air observation from Santa Teresa, NM (figure 20), while not a close proximity sounding, also indicated high relative humidity and weak easterly flow in the middle levels. Surface winds were light from the northeast at LRU at the start of the flight with southeast winds at 3.6 m/s at the conclusion of the flight. The main modeling emphasis on this day was to study how long (in time) and how effective the ingested TAMDAR-U data was in the model output.

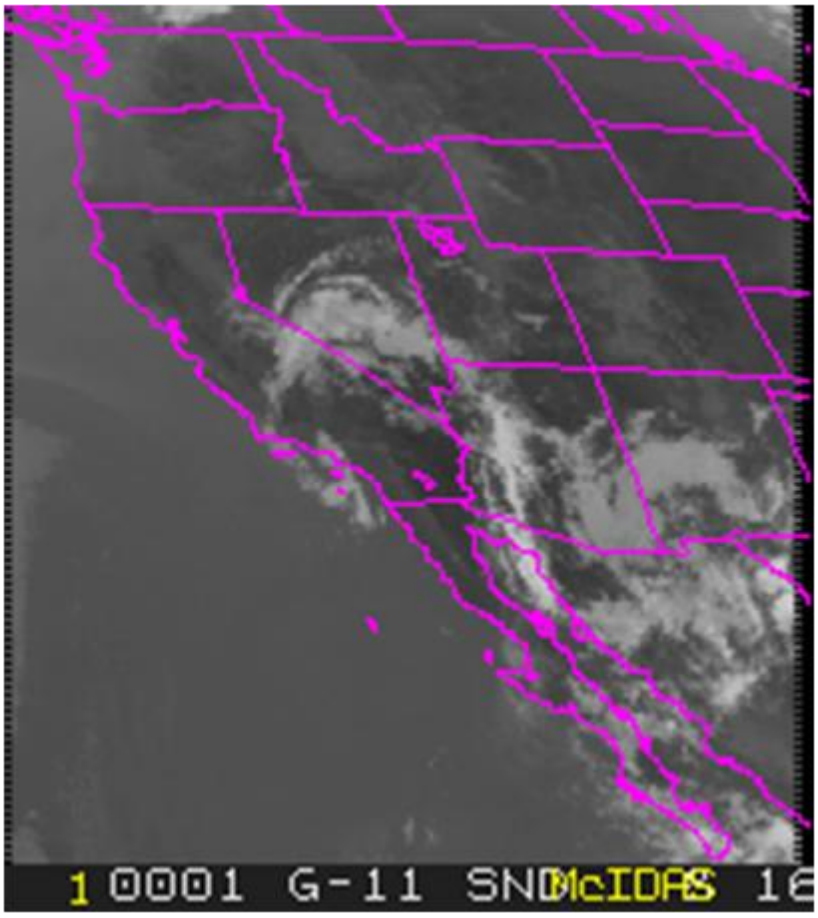

Figure 19. Satellite image over southwestern United States valid at 1601 UTC 16 July 2011.

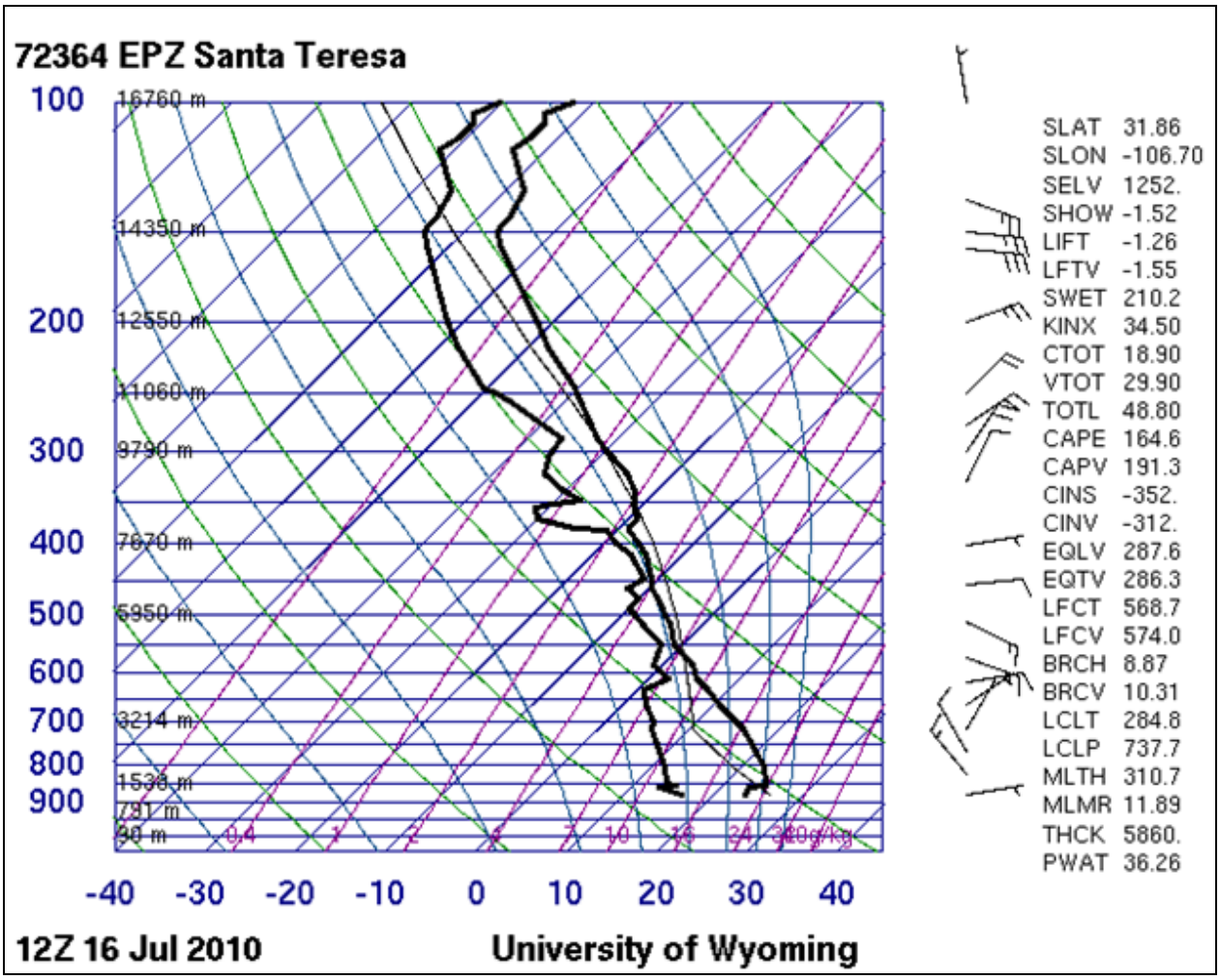

Figure 20. Upper-air observation at 1200 UTC 16 July 2010 from Santa Teresa, NM.

Note: The source for figure 20 is the University of Wyoming, Department of Atmospheric Sciences website (*10*).

At 1700 UTC the Aerostar was located just to the northeast of the Sierra de Las Uvas. The model output at 1700 UTC with and without TAMDAR-U data ingested indicates the wide-ranging pattern of north-to-south wind flow toward the border of Mexico and Texas from 355°. This northerly flow, along with higher cloud cover, tended to enhance and prolong the morning drainage flow off the higher terrain toward the valley locations (not shown). Figures 21 and 22 are very similar, although it appears that the TAMDAR-U data added a stronger flow over the San Andres Mountains on the eastern edge of the domain as shown in figure 22. Furthermore, there appears to be a slightly stronger flow off the higher terrain of the Black Range in the northwest corner of the grid in the case with the TAMDAR-U data ingested.

Two hrs after the Aerostar flight and TAMDAR-U data collection ended, there are minor differences between the two model cases with and without the TAMDAR-U data as can be seen in figures 23 and 24.

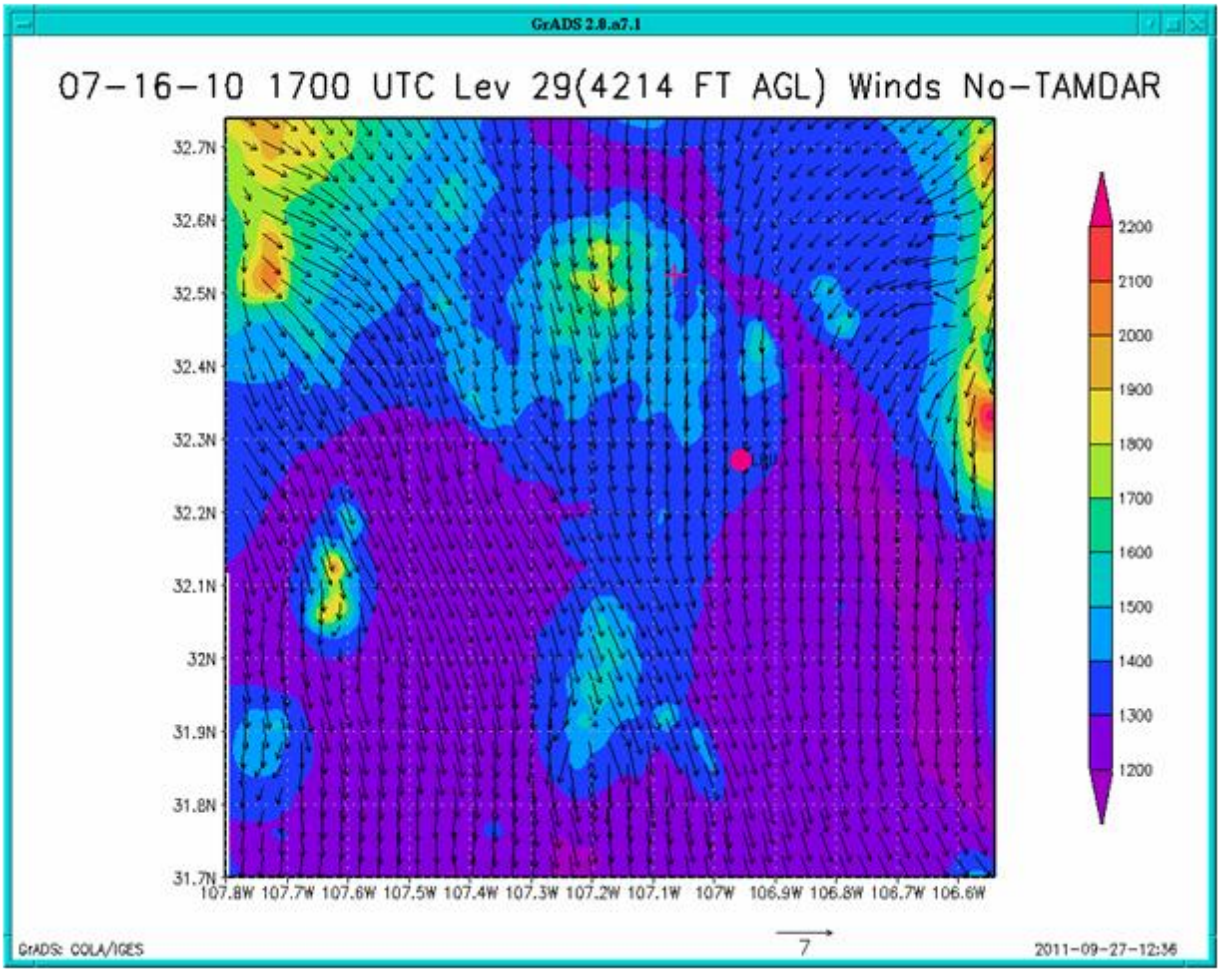

Figure 21. 16 July 2011 1700 UTC WRF wind speed and wind direction forecast at Level 29 (4214 ft AGL) with no TAMDAR-U data.

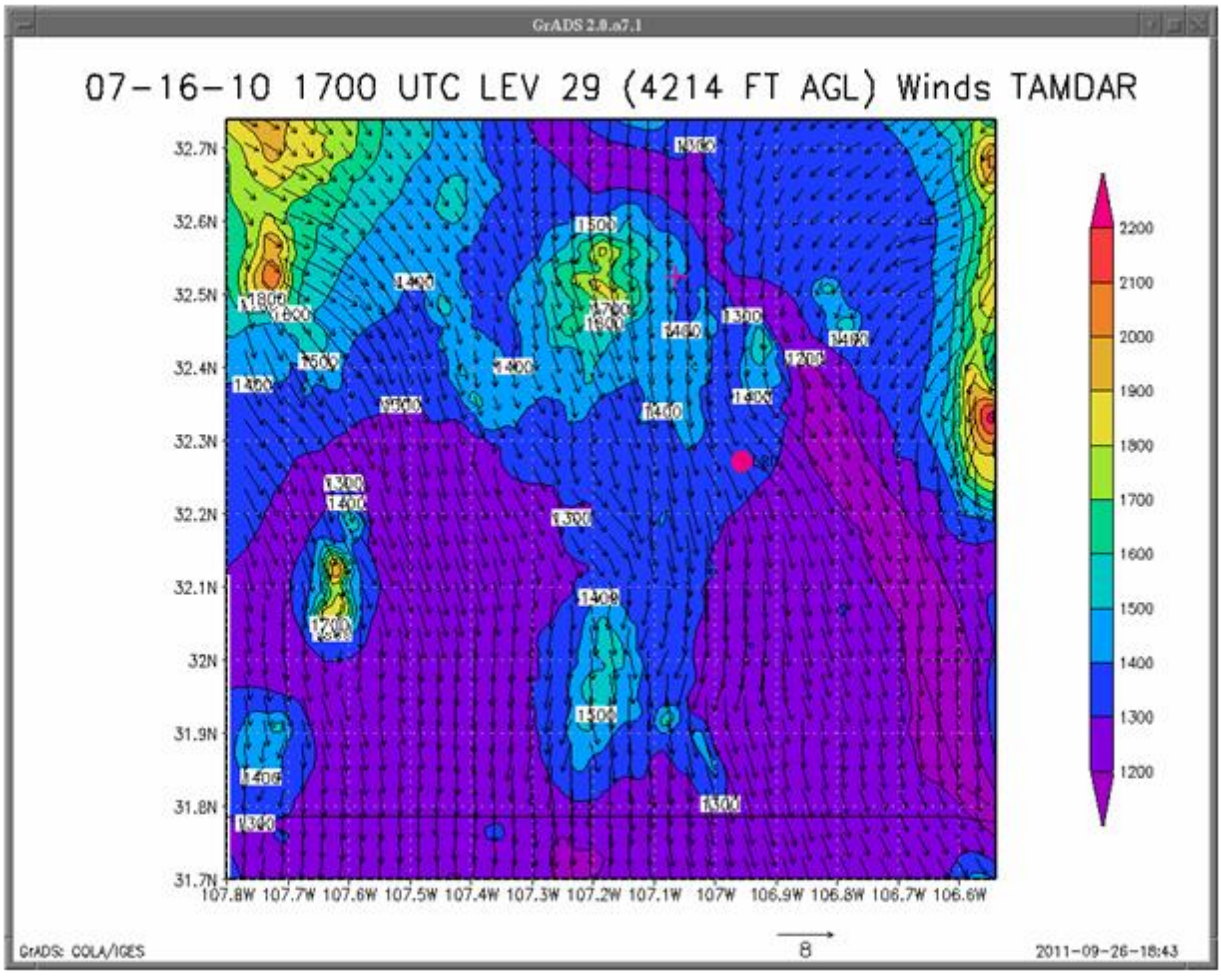

Figure 22. 16 July 2011 1700 UTC WRF wind speed and wind direction forecast at Level 29 (4214 ft AGL) with TAMDAR-U data.

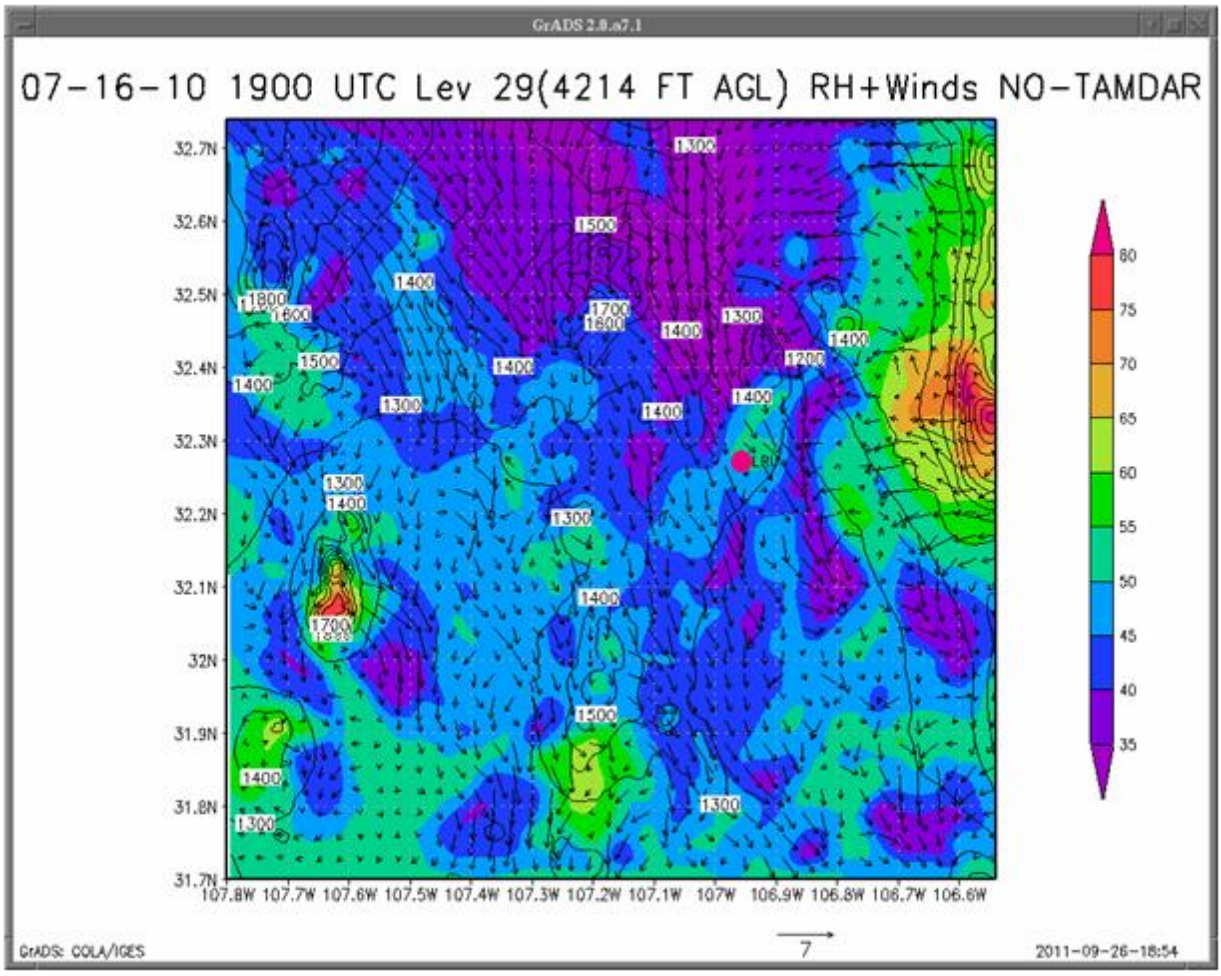

Figure 23. 16 July 2011 1900 UTC WRF relative humidity and wind direction forecast at Level 29 (4214 ft AGL) with no TAMDAR-U data.

There appears to be a slight adjustment in the wind and RH fields in figure 24, which includes the TAMDAR-U input, as can be seen by slightly stronger winds off the Organ Mountains to the east of the flight location. The down-valley (north-to-south) flow seen at 1700 UTC had diminished and the model was forecasting the gradual diurnal change toward localized wind speeds and directions based on the heating of the terrain features on the grid. The model does show the higher RH over the mountain peaks where cooler temperatures prevailed while valley locations had much drier conditions due to the increasing boundary-layer temperatures. One of the intriguing results shown in figures 23 and 24 are that there are more differences in the RH and wind fields away from where the Aerostar was taking readings or downstream in the wind flow. This makes sense when considering the wind speed and wind direction that the TAMDAR-U input would be advected downstream toward the southern part of the grid. In the case without TAMDAR-U input (figure 23) the RH field on the southern part of the grid appears to average about 5% lower than the case with the TAMDAR-U data. Additionally, with the TAMDAR-U data (figure 24), the RH is slightly higher over the high terrain of the local mountain ranges. It is

uncertain if this is due directly from the TAMDAR-U input or is an indirect influence via model advective or diffusive processes.

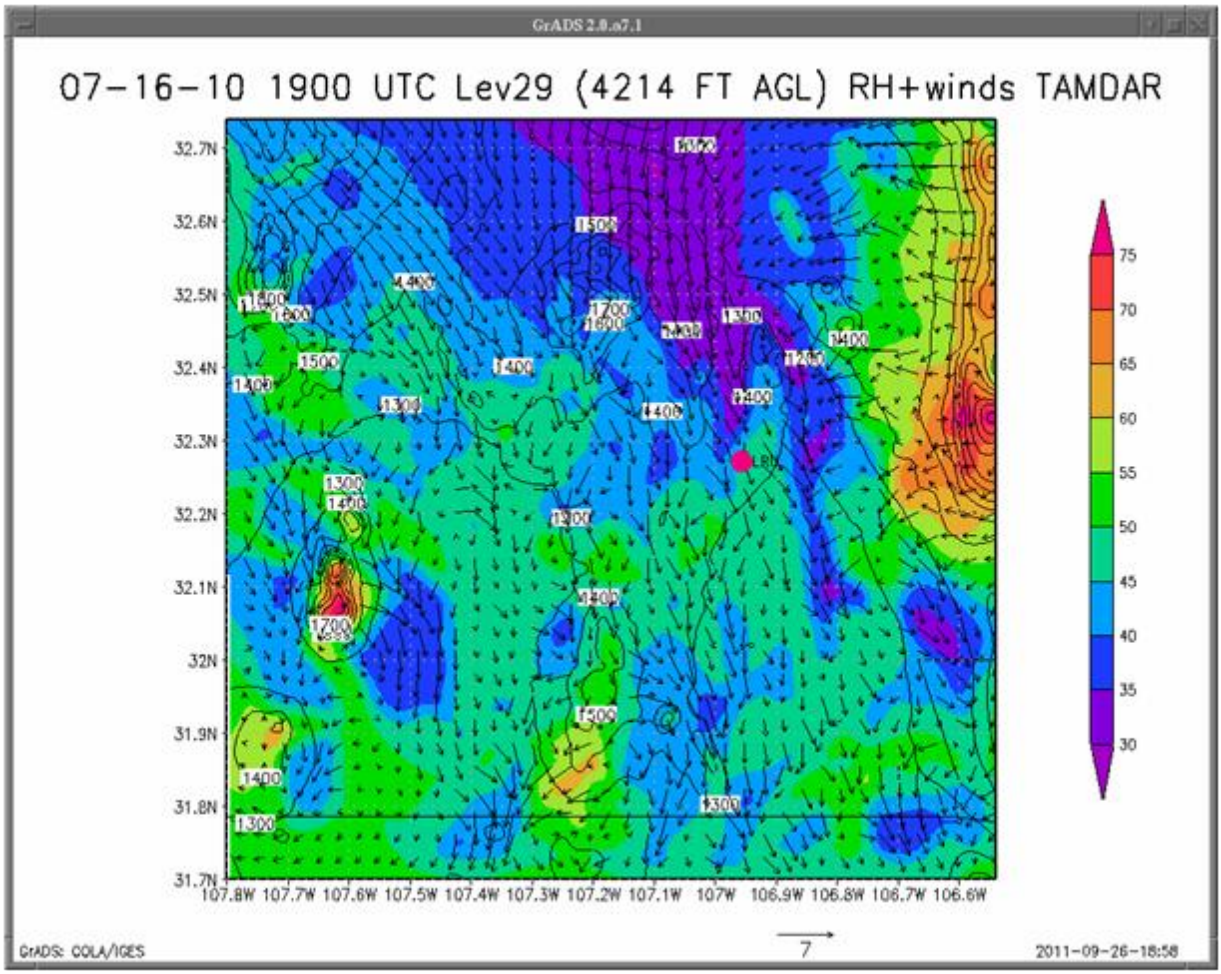

Figure 24. 16 July 2011 1900 UTC WRF relative humidity and wind direction forecast at Level 29 (4214 ft AGL) with TAMDAR-U data.

Three hrs later, at 2200 UTC, figure 25 (without TAMDAR-U) and figure 26 (with TAMDAR-U data), show the same general trends. These two figures are focused more into the flight area; there appears to be an area of lighter wind near the eastern mountains in the TAMDAR-U case with slightly higher RH values noted on the southern edge of the plot and the higher terrain.

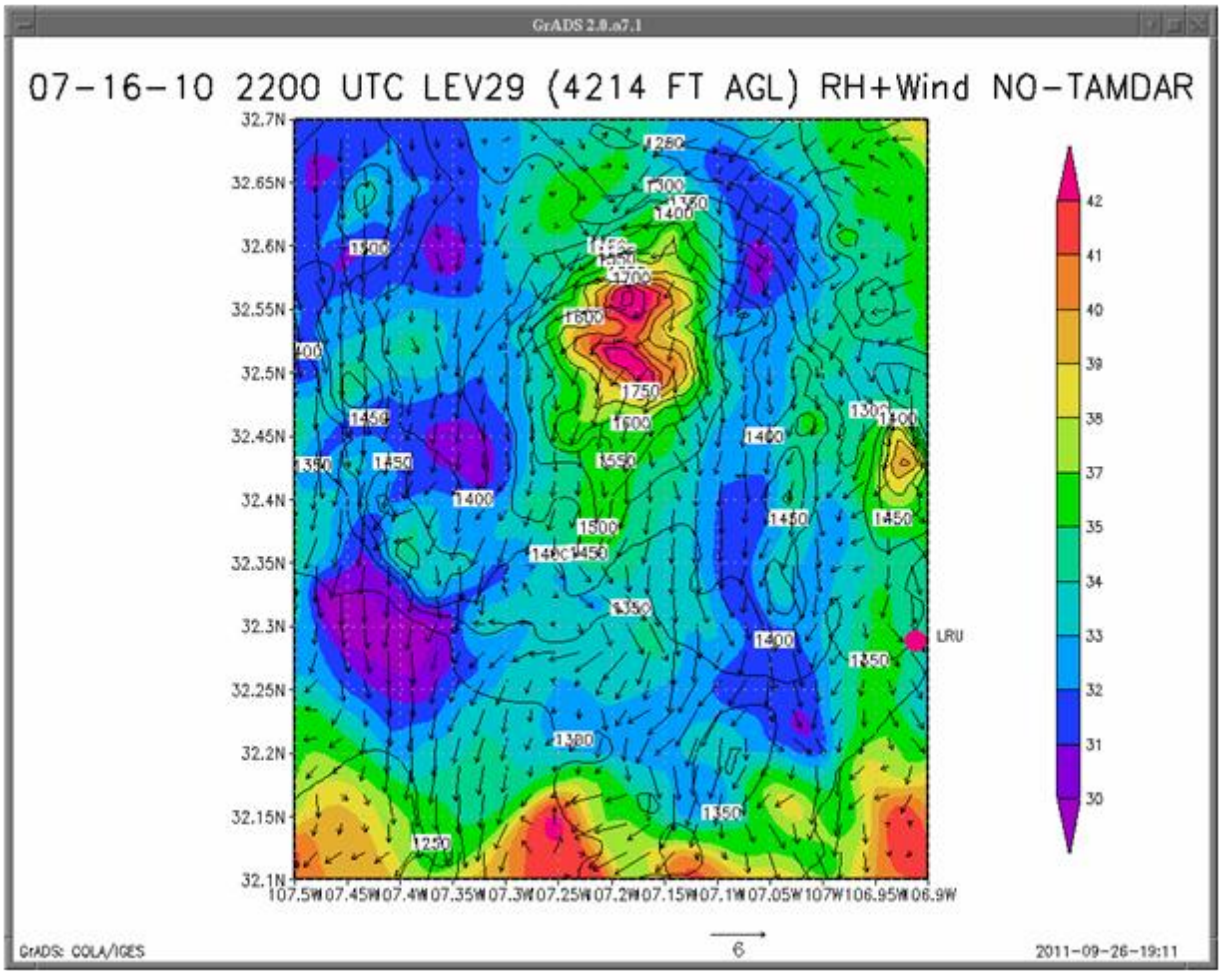

Figure 25. 16 July 2011 2200 UTC WRF relative humidity and wind direction forecast at Level 29 (4214 ft AGL) with no TAMDAR-U data.

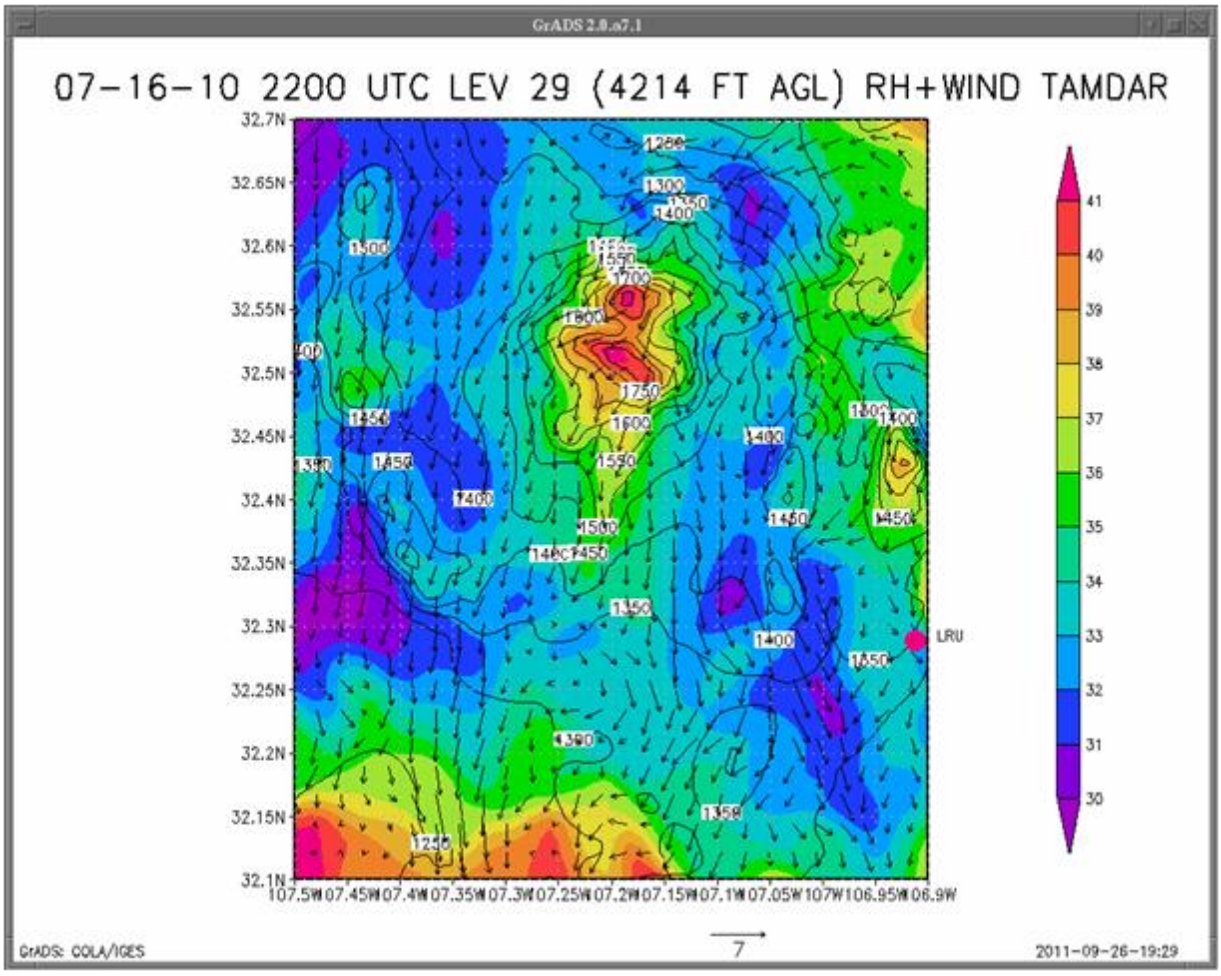

Figure 26. 16 July 2011 2200 UTC WRF relative humidity and wind direction forecast at Level 29 (4214 ft AGL) with TAMDAR-U data.

The final plots shown for the 16 July case are plots of precipitation without (figure 27) and with TAMDAR-U (figure 28) data. These plots are from the final hour of the model run, 0100 UTC 17 July, which is 8 hrs after the flight and data ingest were completed. While it can be assumed the TAMDAR-U data have little direct influence in the model output at this hour, it still accumulates precipitation over the late afternoon hours with a very slight shift in the forecast in the two cases. The difference between 0.03 (in) and 0.06 (in) is insignificant, but it does show that changes in the wind field or thermodynamics caused by ingesting TAMDAR-U data do create differences in the precipitation output in this model run.

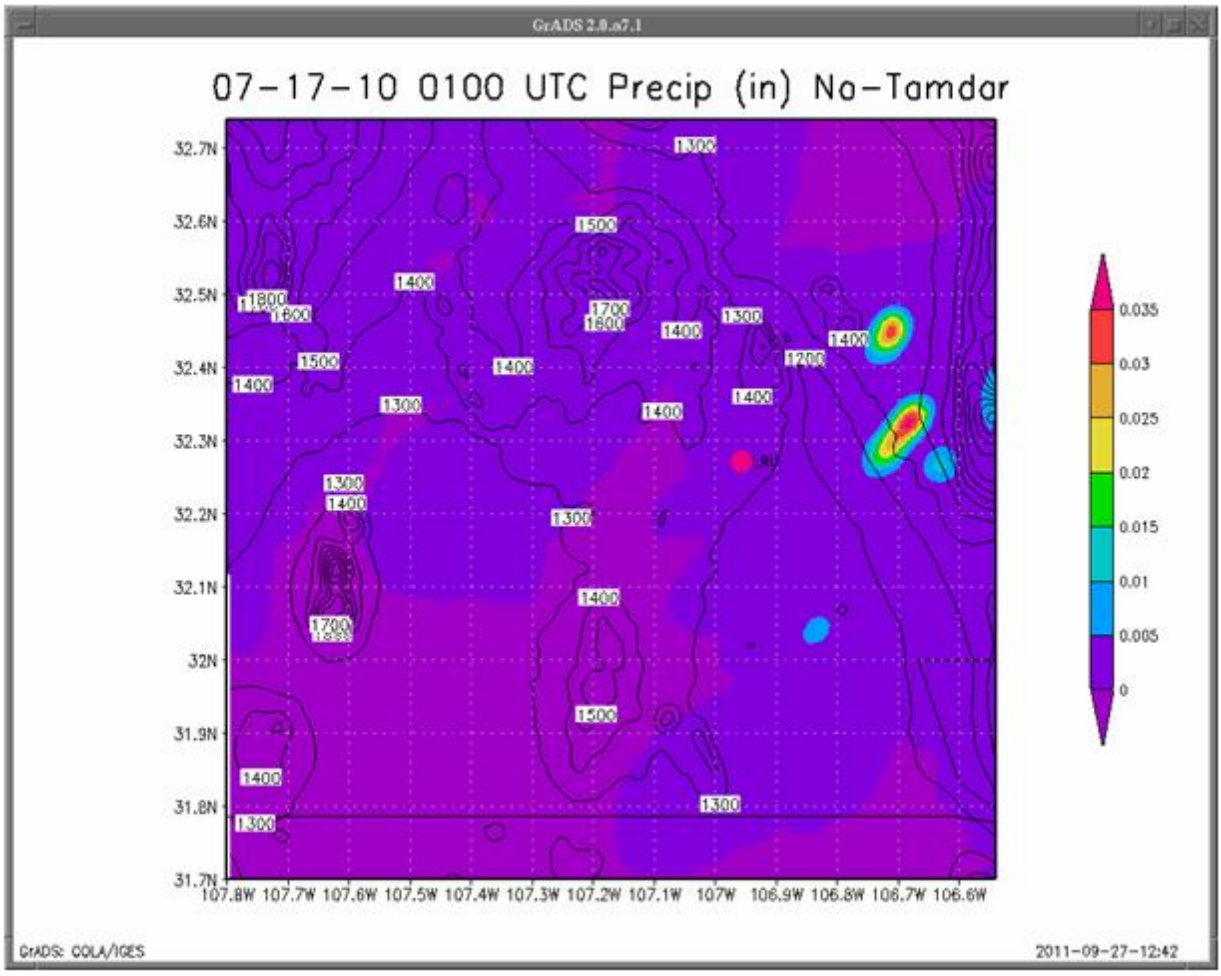

Figure 27. 17 July 2011 0100 UTC WRF precipitation (in) forecast with no TAMDAR-U data.

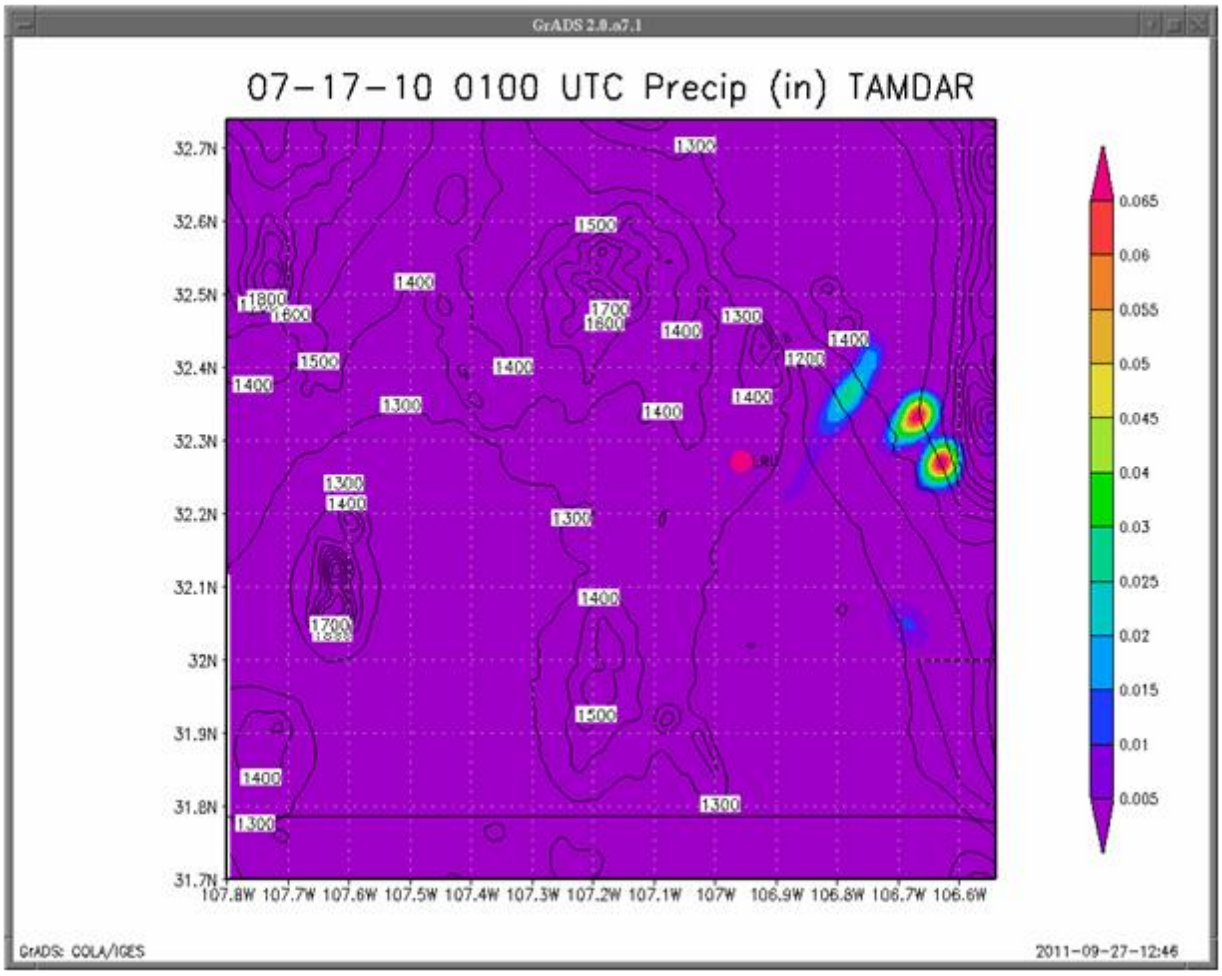

Figure 28. 17 July 2011 0100 UTC WRF precipitation (in) forecast with TAMDAR-U data.

Another way to look at the influence of FDDA is looking at the forecasted RH and cloud forecasts. To visualize this, the Paraview software was used to show a comparison between the FDDA and control case for 0100 July 16 2010 over the domain. Figure 29 is for the control case and figure 30 is for the FDDA case. As has been the trend with many of these meteorological variables, the discrepancies between the two plots are difficult to pinpoint, but they do show up in the cloud forecasts, which are dependent on the RH and the vertical motions field, even 8 hrs after the data ingest has terminated. There are some areas where the "cloud" formations are enhanced in the FDDA case with the TAMDAR-U data included. This may be due to a response in the temperature field, moisture field, or vertical motion field.

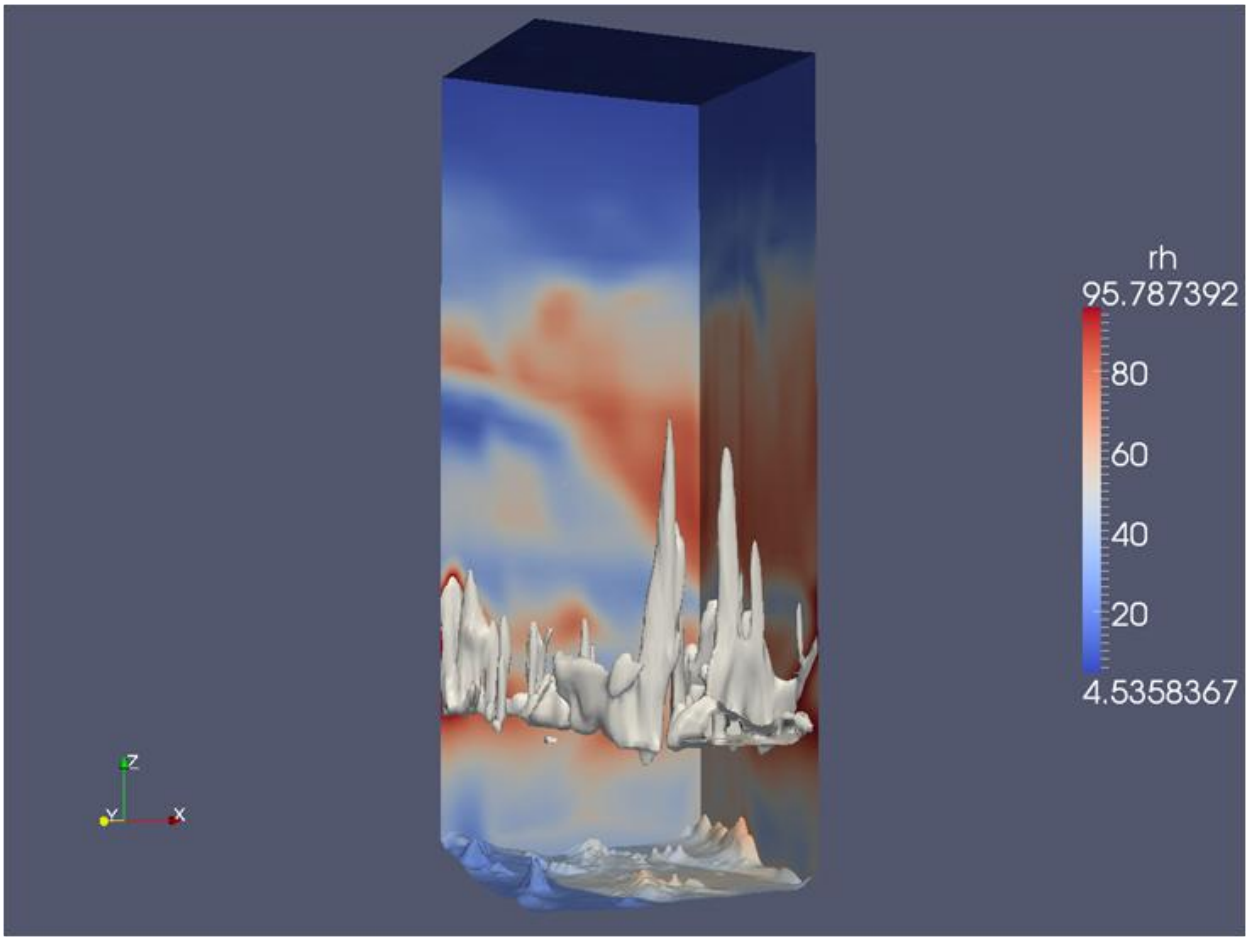

Figure 29. Paraview image for 0100 UTC 16 July 2010 showing the forecasted RH and clouds for the control run, where no TAMDAR-U data was ingested in the model.

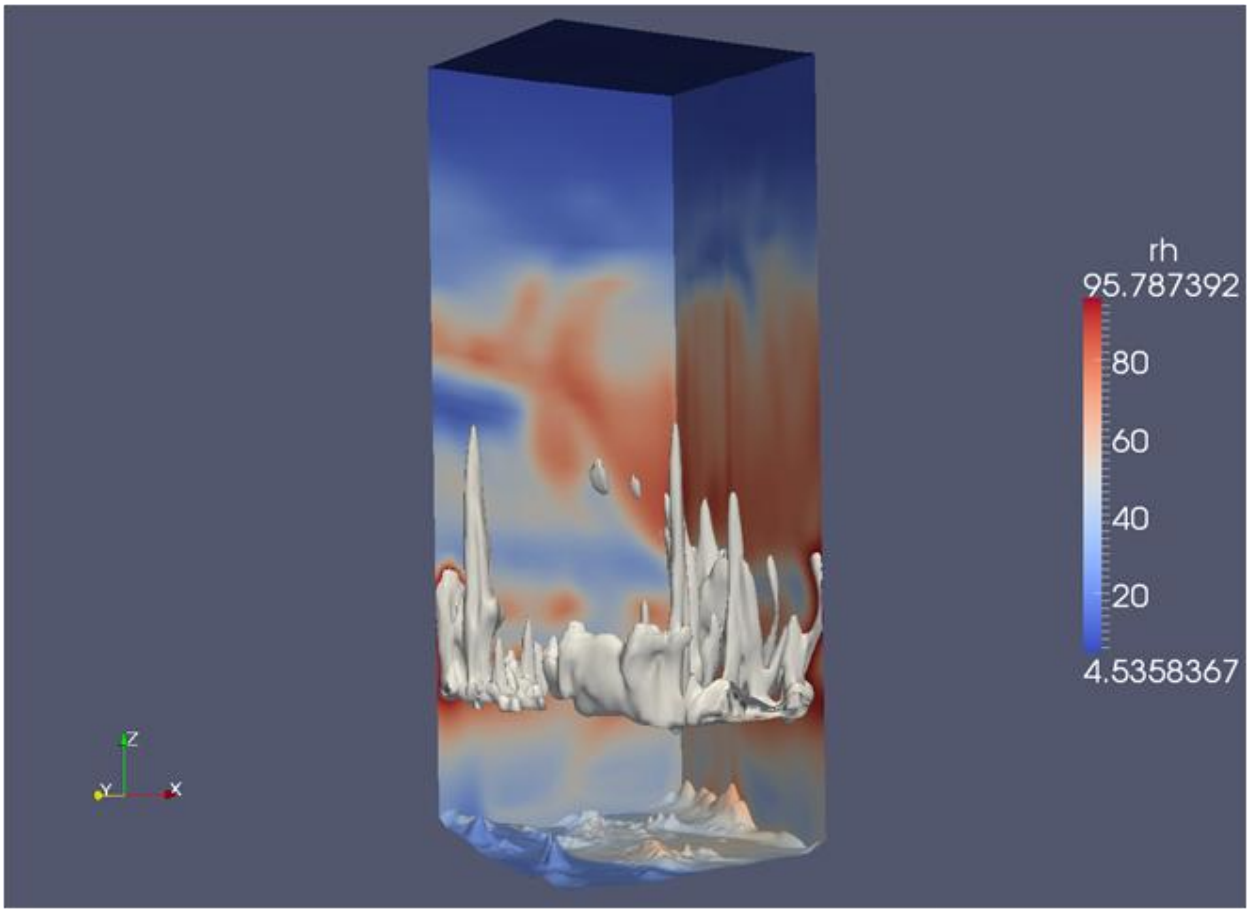

Figure 30. Paraview image for 0100 UTC 16 July 2010 showing the forecasted RH and clouds for the case where TAMDAR-U data was ingested into the WRF.

Another part of the study was to compare an upper-air sounding taken at 2027 UTC at LRU against the model output at the same time.[1] In figure 31 the WRF model plot includes no TAMDAR-U data; however, in figure 32 the plot does include the TAMDAR-U data in the WRF. The blue line (dew point) and the black line (temperature) are from the LRU sounding, while the purple line (dew point) and red line (temperature) are WRF model output. The orange wind barbs are from the WRF model while the black wind barbs are from the LRU 2027 UTC sounding. The temperature plots are nearly identical. The same trend is seen with the dew point plot, although there is moister air observed by the Rawinsonde Observation below 600 hPa and drier air between 600 hPa to 500 hPa than the model had forecasted. While it is difficult to see, the wind barbs (directions) are generally the same with and without the TAMDAR-U data. It is unfortunate that the low-level winds could not be verified in this case but the winds are from the northeast with a layer of northwest flow above and then a shift back to northeast above 700 hPa, which does agree with the available sounding wind data.

[1] On this case-study day, it was possible to obtain a complete sounding of thermodynamic data from the LRU site during the model forecasting period; however, the wind data were incomplete.

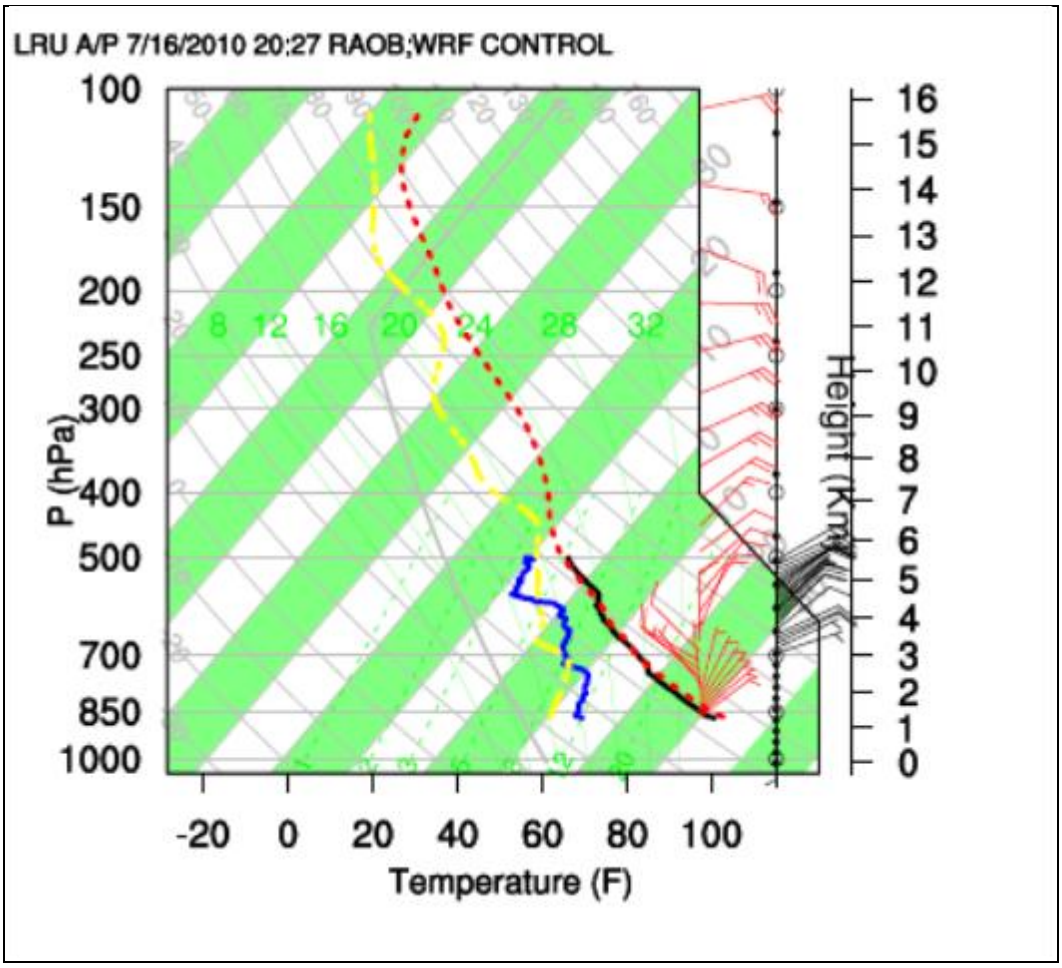

Figure 31. 16 July 2011 2027 UTC WRF forecast sounding no FDDA data and observed upper-air data from LRU.

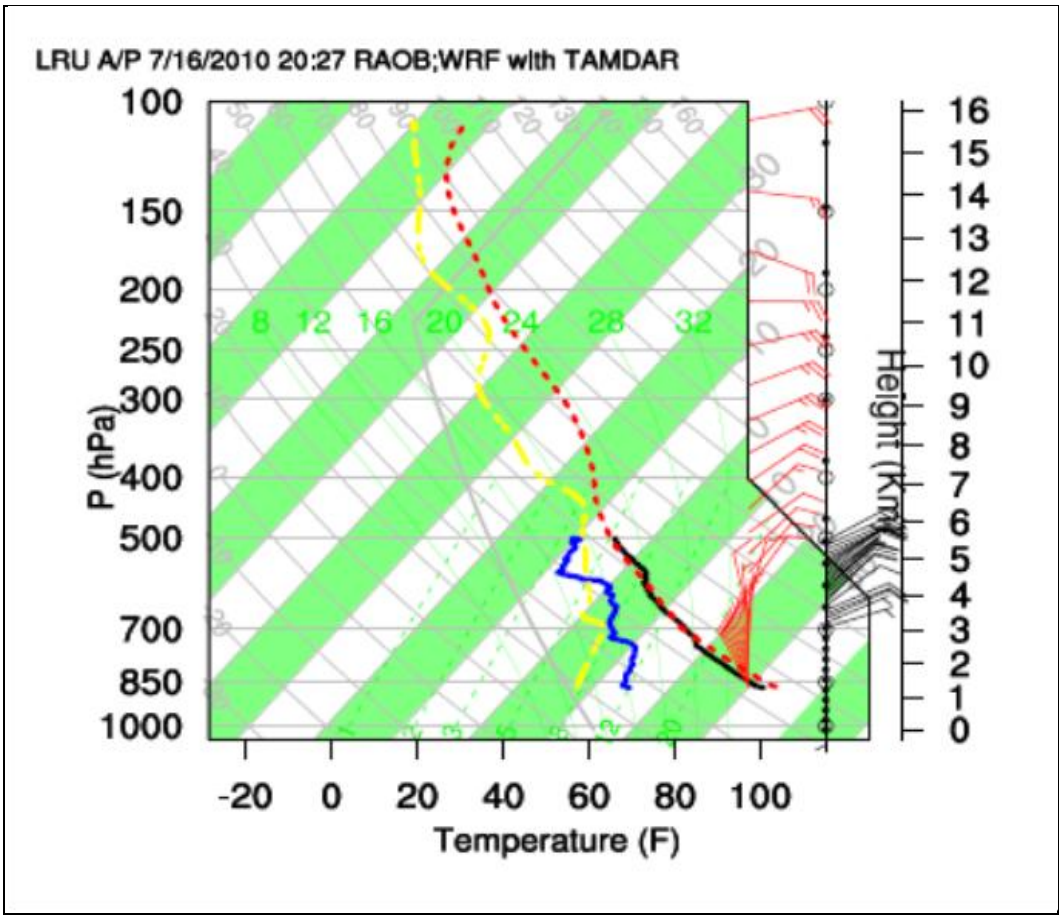

Figure 32. 16 July 2011 2027 UTC WRF forecast sounding TAMDAR-U data and observed upper-air data from LRU.

6. Case Study 3: 20 August 2010

The morning weather on 20 August was tranquil with clear skies and light northerly surface winds. In figure 33, the satellite photo indicates minimal cloud cover over the western United States as the center of an upper ridge was over New Mexico with sinking vertical motions. The upper-air sounding taken at the Santa Teresa, NM airport (not shown) at 1200 UTC indicated surface winds from the south, with a layer of southwest to west winds above to 700 hPa with winds speeds 5 to 7 m/s. Above 700 hPa winds were light and variable as would be expected under a large upper ridge.

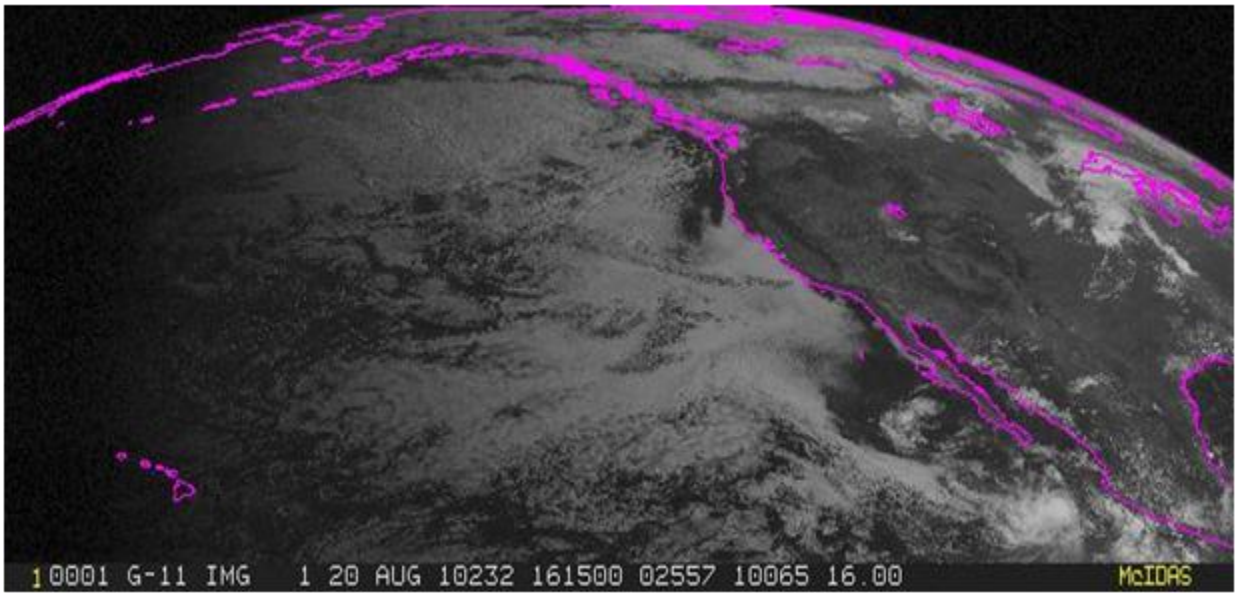

Figure 33. Satellite from 20 Aug 2010 at 1615 UTC.

Note: The source for figure 33 is the Digital Cadastral Databases (DCDBS) website (*11*).

At 1700 UTC, the Aeroostar was located almost due west of LRU and flying at a height of 5272 ft AGL. TAMDAR-U data indicated a temperature of 17.2 °C at 1700 UTC. Figure 34 shows the temperature field without TAMDAR-U data while figure 35 displays the temperature over the domain with TAMDAR-U assimilated into the model.

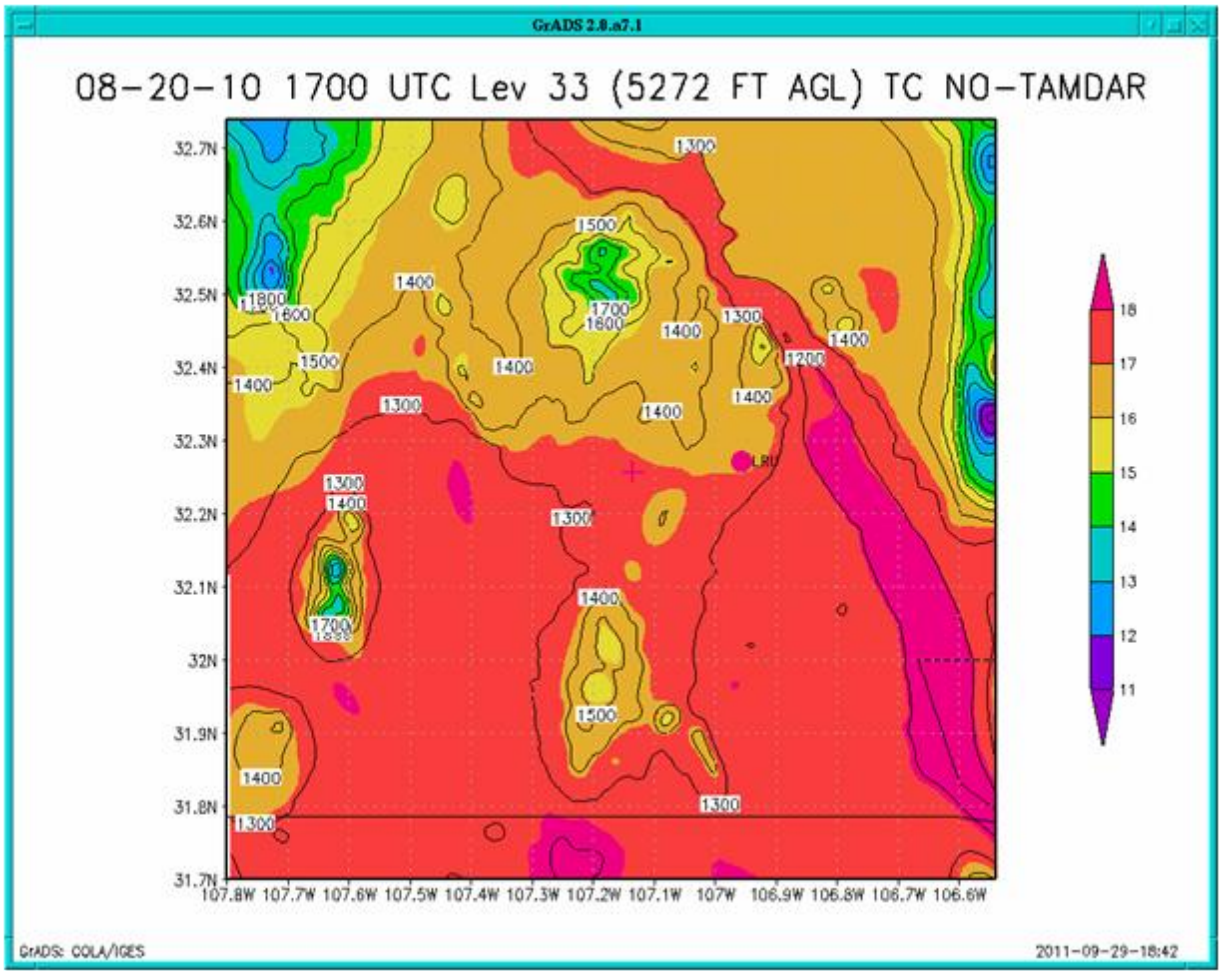

Figure 34. 20 August 2010 1700 UTC WRF temperature (°C) forecast without TAMDAR-U data.

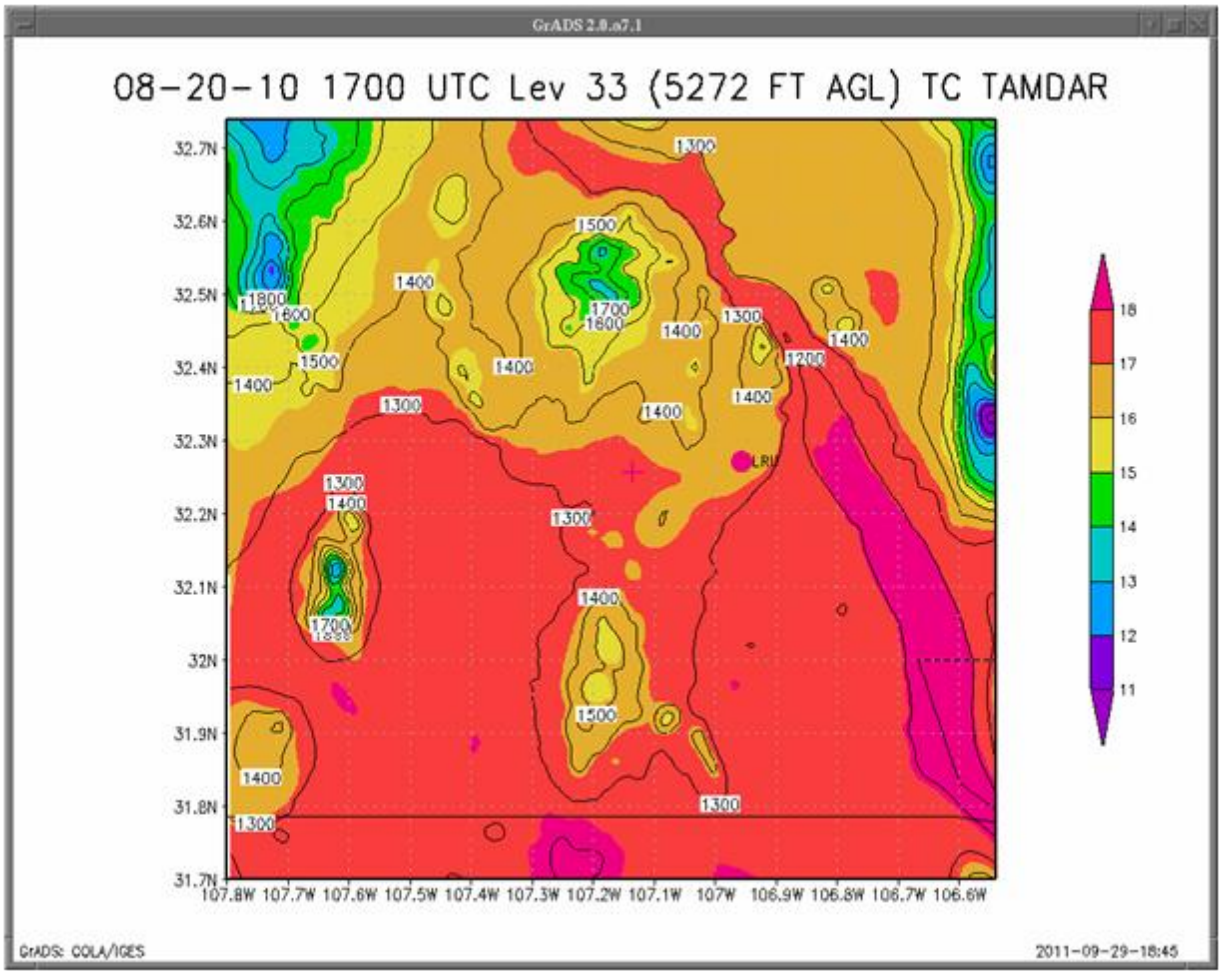

Figure 35. 20 August 2010 1700 UTC WRF temperature (°C) forecast with TAMDAR-U data.

Based on the model forecasts, the temperatures are almost identical with only slight variations at a few grid points.

The most interesting meteorological field appears to be for the RH. Figure 36 shows the RH field at 1500 UTC at Level 33 (5272 ft AGL) before the Aerostar flight began at 1538 UTC. Typical for a summer day, the highest relative humidity was over the higher terrain and the lowest was in the valley where sunshine was warming the atmosphere.

Once the flight began and TAMDAR-U data were collected and assimilated into the model, the 1600 UTC plot became rather complex as the Aerostar circled northeast of LRU and then slowly moved to the northwest of the airport and increased height quickly after 1600 UTC. The UAS was located at 3132 ft AGL at 1600 UTC, but reached the flight level of about 5272 ft AGL shortly after 1600 UTC. The forecasted 1600 UTC RH and wind field are displayed in figure 37 with the TAMDAR-U data included. While the RH differences are not significant between the control run (not shown) and the FDDA run, they do indicate a slight increase in RH that was experienced along the UAV flight path from the northeast to northwest of LRU.

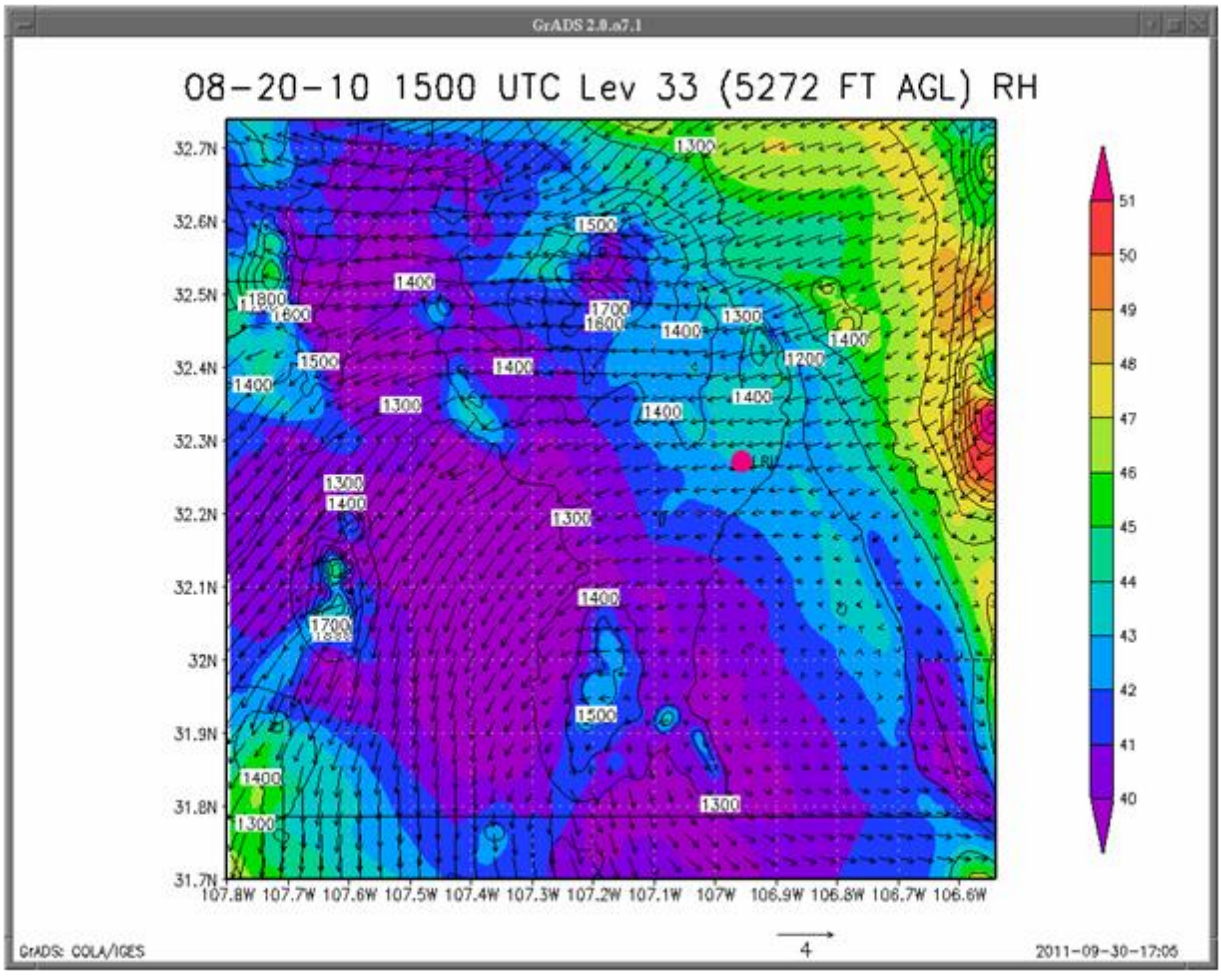

Figure 36. 20 August 2010 1500 UTC WRF RH and wind forecast at Level 33 (5272 ft AGL) before the flight.

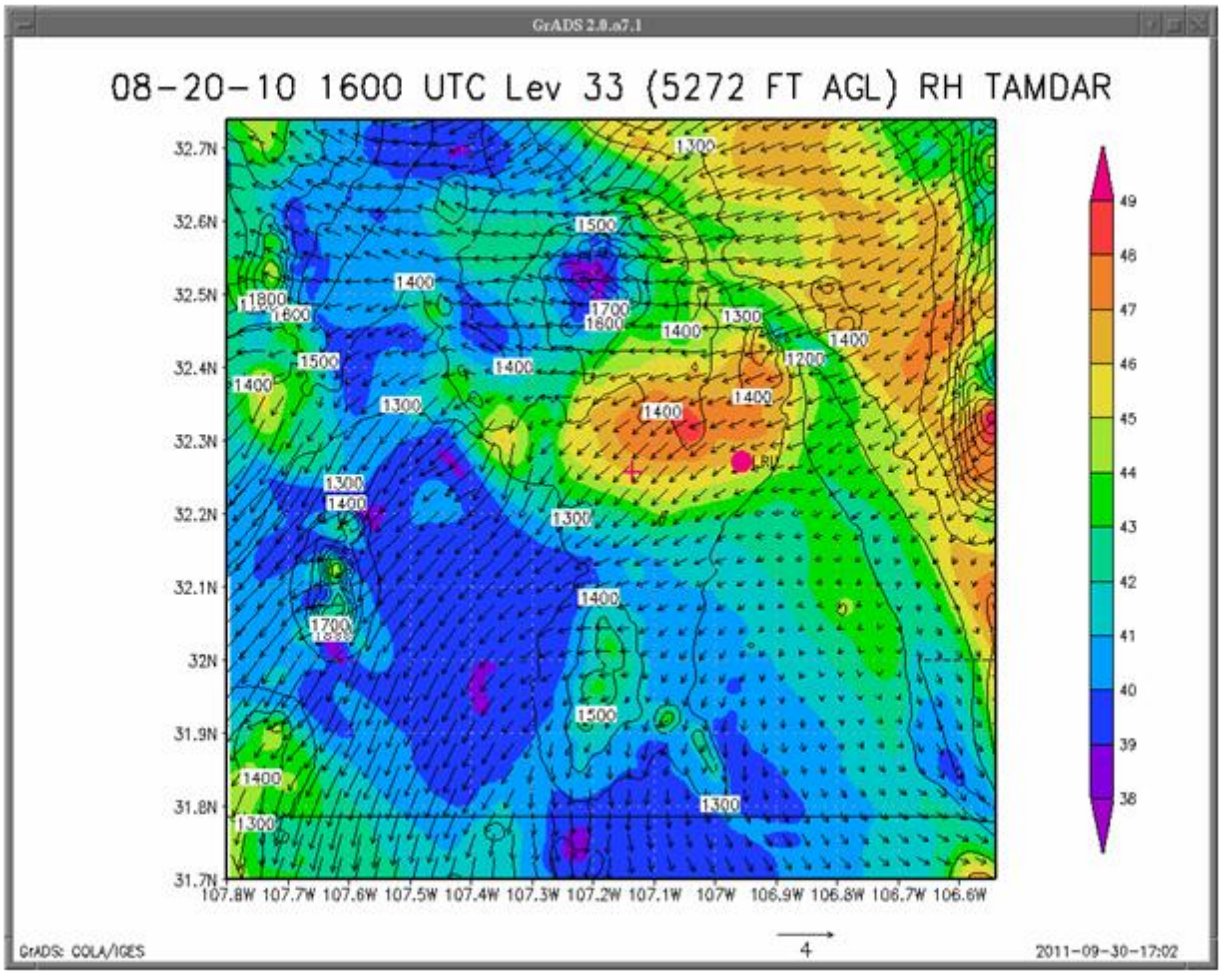

Figure 37. 20 August 2010 1600 UTC WRF RH and wind forecast at flight level (5272 ft AGL) with TAMDAR-U data.

From 1600 to 1700 UTC, the Aerostar flew from LRU to the SW near the Florida Mountains in the southwest corner of the grid. Then it turned around and by 1700 UTC, the Aerostar was located due west of LRU at 107.13 W longitude. Thus, these data far away from LRU did not get assimilated into the 1700 UTC data because it was beyond the radius of influence. However, data near the Aerostar location was incorporated into the model solution where higher RH values are forecasted just north of the airport as shown in figure 38. Another view of this is shown in figure 39, where the larger Domain 1 is shown at 1700 UTC. Only the location of the Aeorstar is shown in this figure, since it is so close to LRU in preparation for landing at 1721 UTC. The slightly higher forecasted RH values can be seen in the blue area of figure 39.

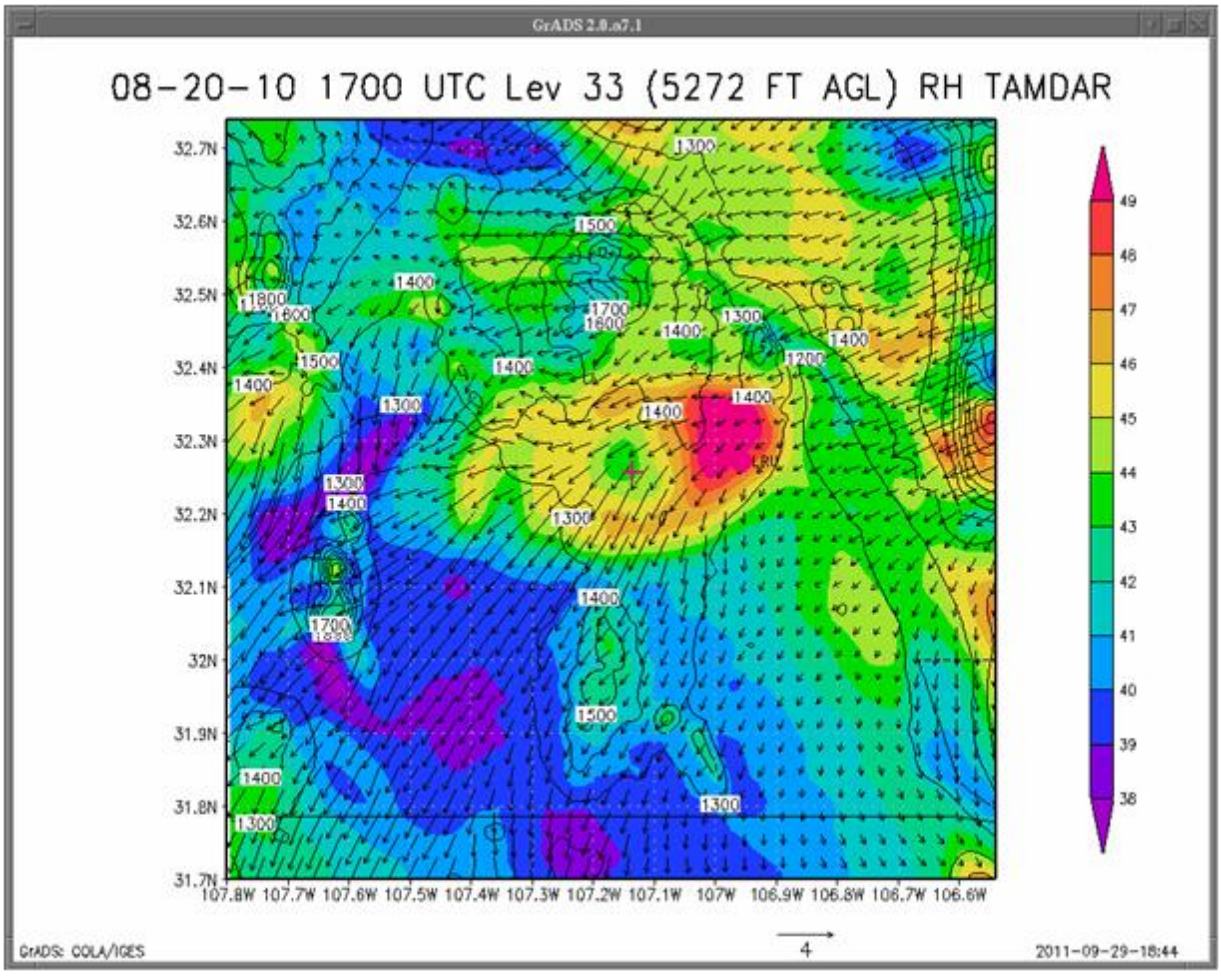

Figure 38. 20 August 2010 1700 UTC WRF RH and wind forecast at 5272 ft AGL with TAMDAR-U data included in the model solution.

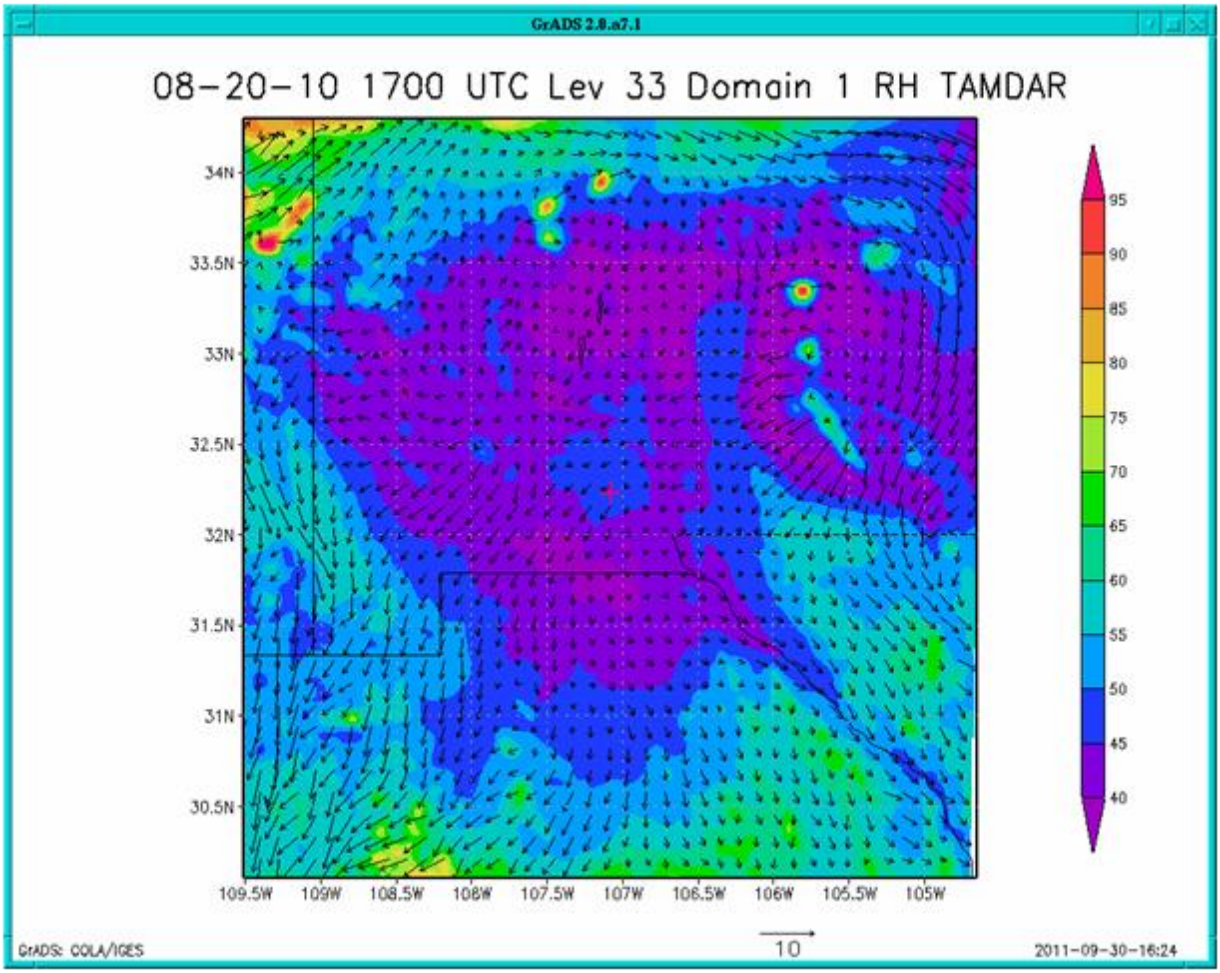

Figure 39. 20 August 2010 1700 UTC WRF RH and wind forecast at 5272 ft AGL with TAMDAR-U data on Domain 1.

The impact of ingesting TAMDAR-U data on the RH and wind fields can still be seen at 1800 UTC (figure 40), 2000 UTC TAMDAR-U (figure 41) and 2000 UTC NO TAMDAR-U (figure 42).

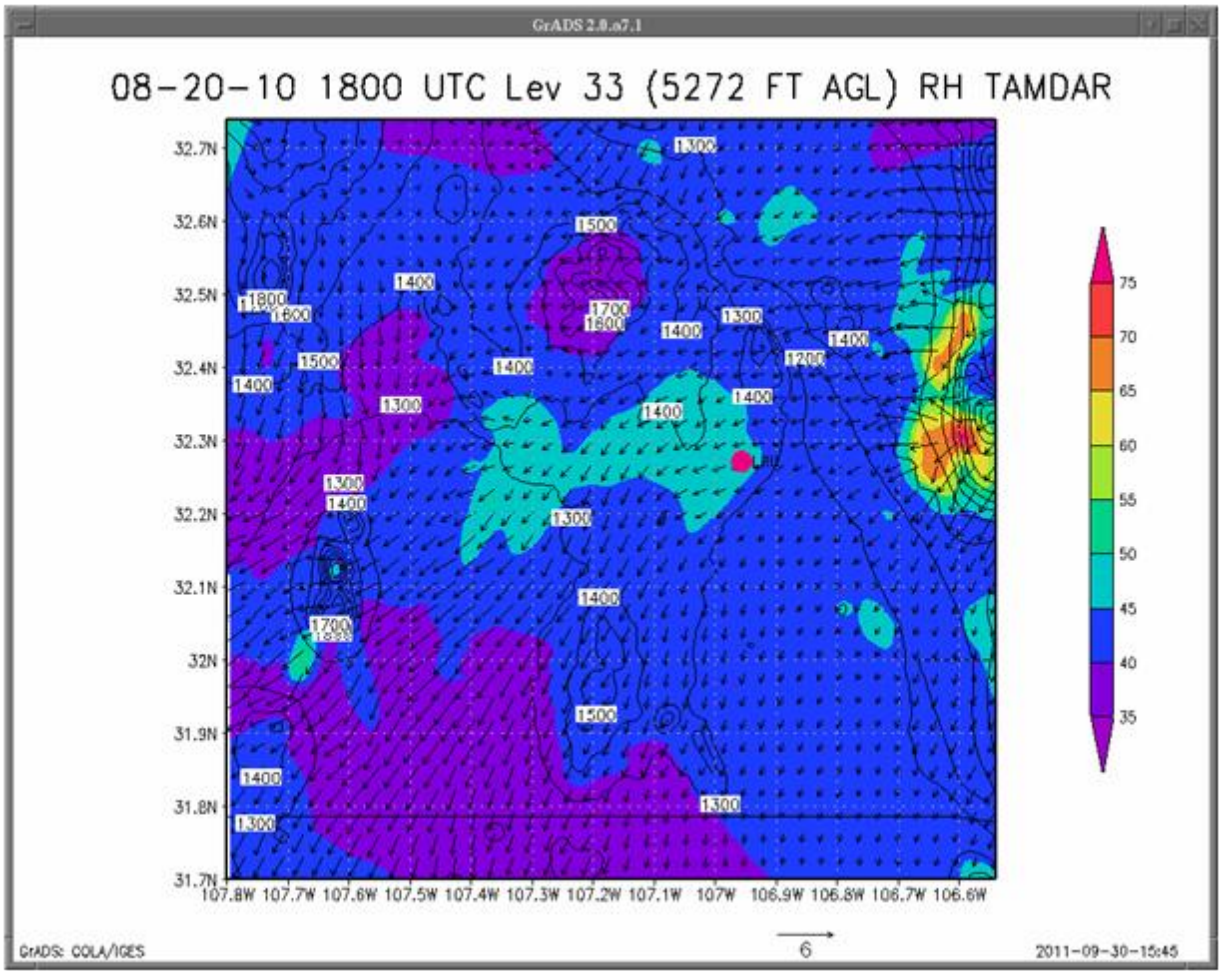

Figure 40. 20 August 2010 1800 UTC WRF RH and wind forecast with TAMDAR-U data.

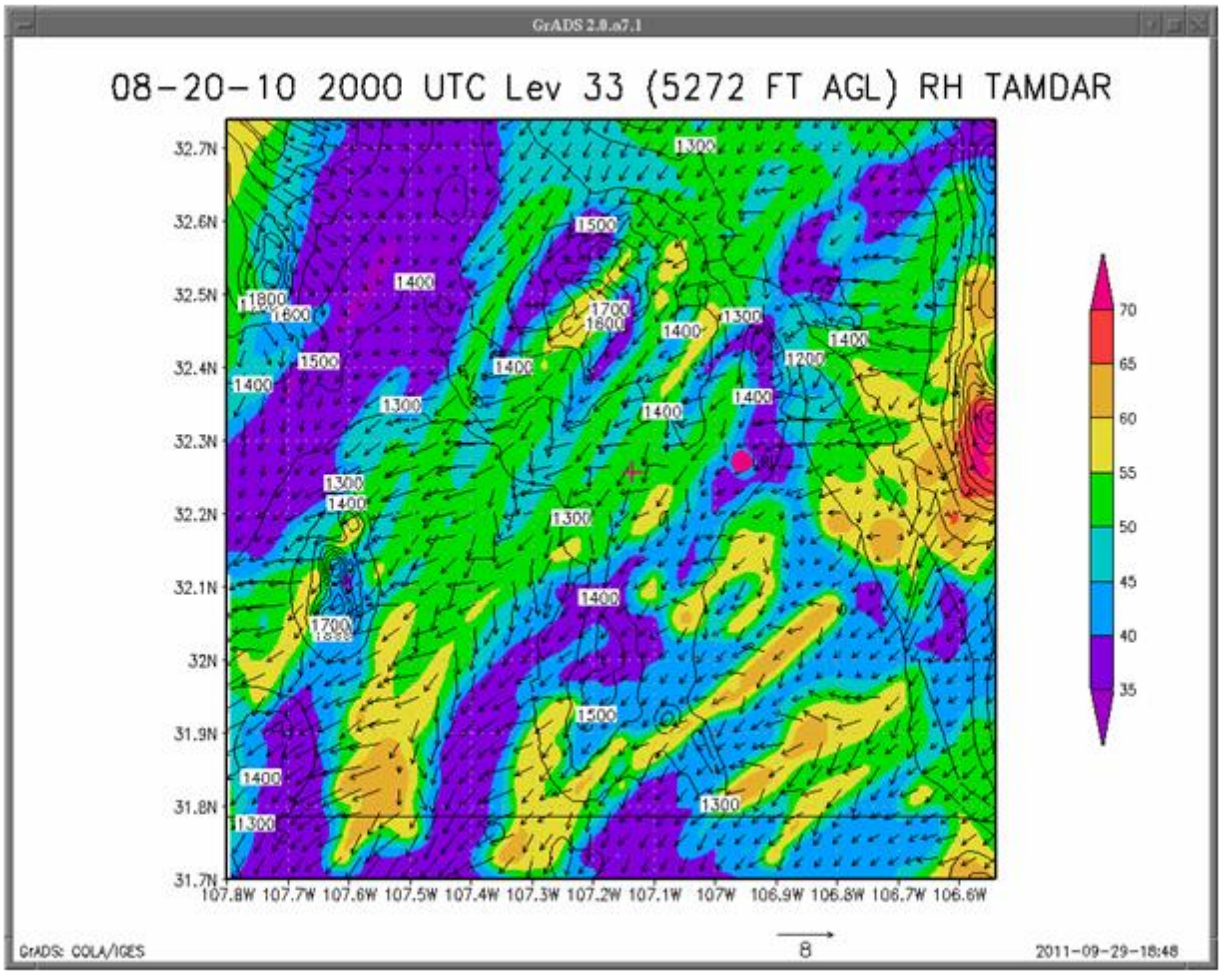

Figure 41. 20 August 2010 2000 UTC WRF RH and wind forecast at 5272 ft AGL with TAMDAR-U data.

By 2000 UTC, a comparison of figure 41 (with TAMDAR-U data) and figure 42 (no TAMDAR-U data), shows only minor differences in any of the tested fields. While it may appear that higher RH has been advected downstream by the wind in figure 41, the same feature appears in figure 42 and may be due to convection or fluxes in the boundary layer.

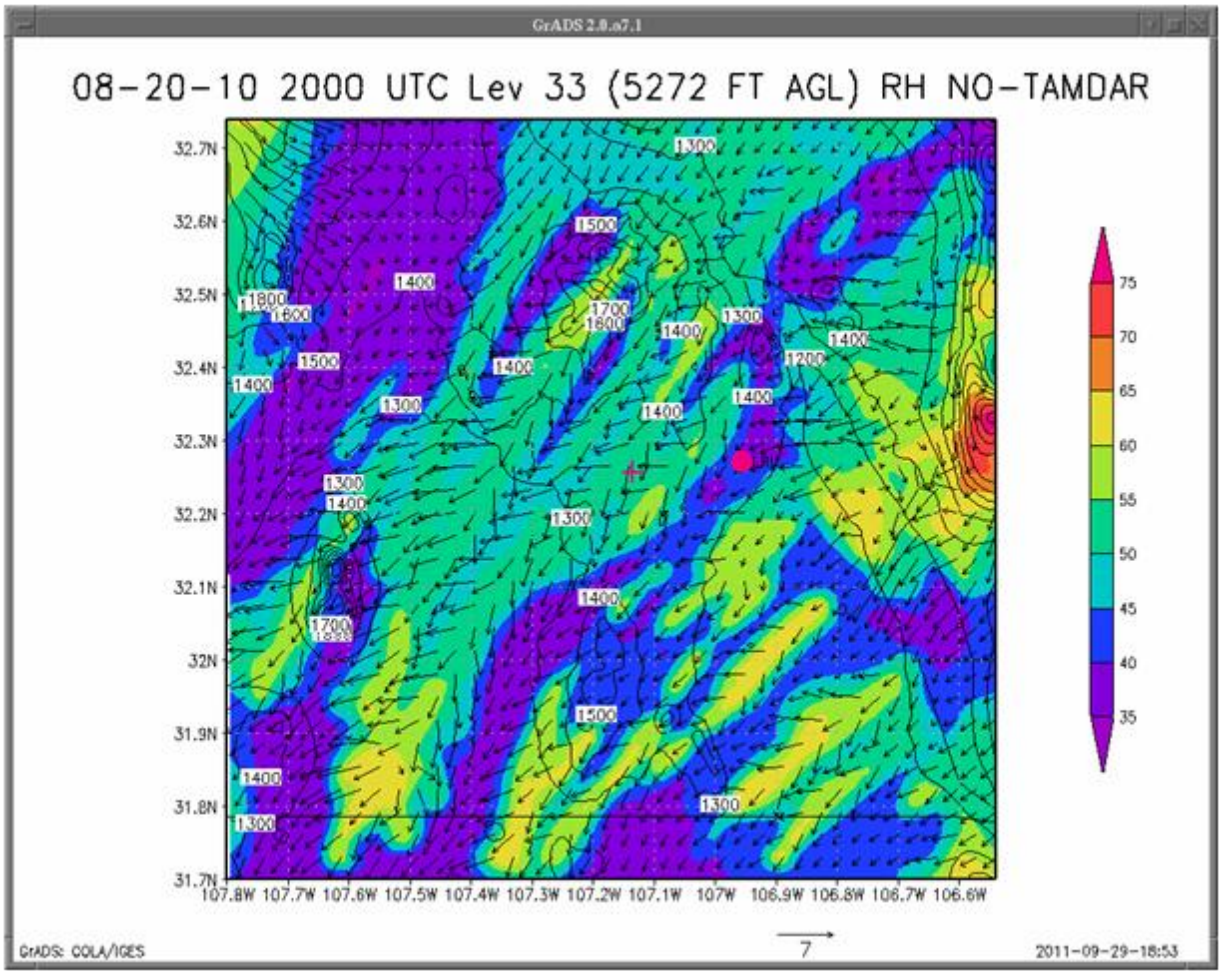

Figure 42. 20 August 2010 2000 UTC WRF RH and wind forecast at 5272 ft AGL with no TAMDAR-U data.

An upper-air sounding was taken by ARL meteorologists at 1954 UTC at LRU and is compared to the WRF forecast at the same time without TAMDAR-U data and with TAMDAR-U data included. The blue line (dew point) and the black line (temperature) are from the LRU sounding, while the purple line (dew point) and red line (temperature) are WRF model output. The orange wind barbs are from the WRF model while the black wind barbs are from the LRU 1954 UTC sounding. As seen in figures 43 and 44, the WRF forecasted temperature field agrees well with the sounding, although the observed dew points are slightly moister in the sounding. These differences in moisture are insignificant. The main disparity between the forecast and the sounding are in the lower-level wind fields. The observed sounding winds are from the south while the forecasted winds from the WRF are from the northeast from the surface to 700 hPa. The model runs shown are over 2 hrs after the flight completed and there is no difference in and of the fields between the case with and without TAMDAR-U data.

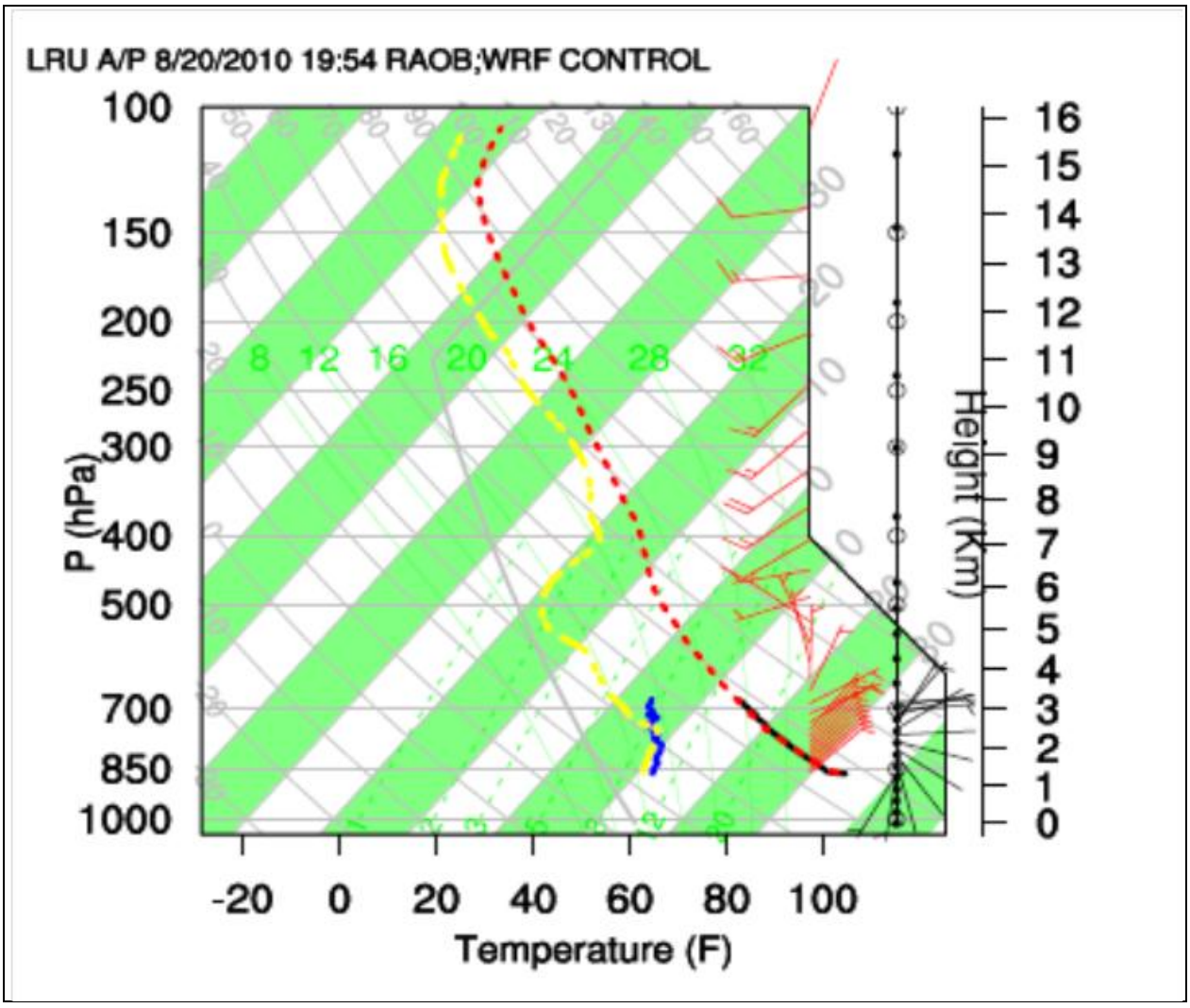

Figure 43. Upper-air observation taken at LRU at 1954 UTC is compared to the WRF control forecast (no TAMDAR-U) at 2000 UTC.

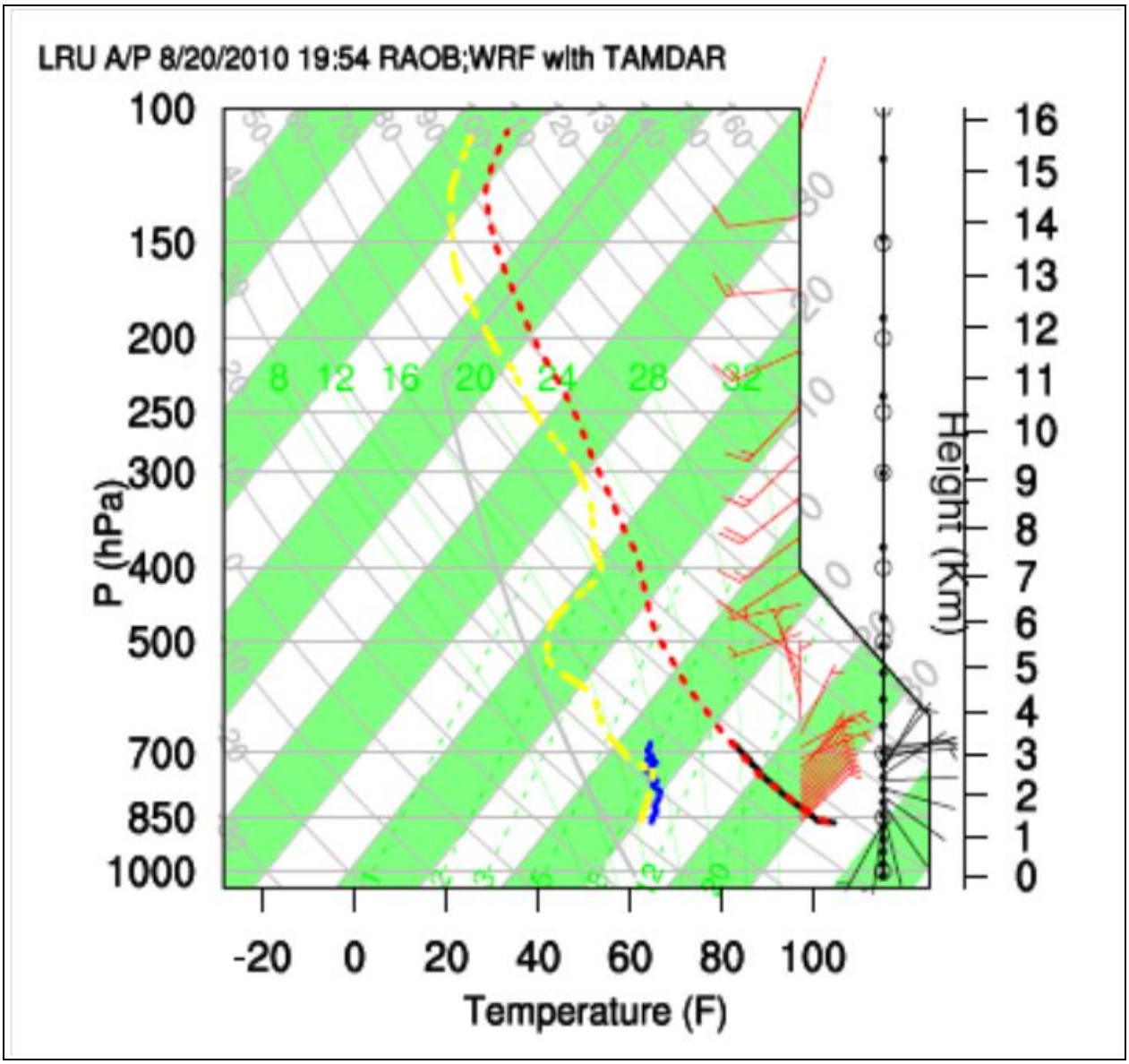

Figure 44. Upper-air observation taken at LRU at 1954 UTC is compared to the WRF forecast with TAMDAR-U data at 2000 UTC.

7. Discussion

There have been numerous studies and research efforts involving FDDA and applications toward different parameters in mesoscale models. It should be noted that FDDA observation nudging can ingest only direct weather observations such as temperature, humidity, winds and pressure-not indirect quantities such as satellite radiance or radar radial velocity or reflectivity like in variational or ensemble Kalman filter assimilation systems. On the other hand, FDDA nudging is

much more computationally efficient and simpler to understand and incorporate, and it does share many commonalities with variational approaches.

One study of FDDA nudging was performed by Stauffer et al. (*12*) who developed and evaluated FDDA in the Pennsylvania State University/NCAR Mesoscale Model (MM5). They showed that use of only coarse-resolution rawinsonde observations through model integration, rather than at the initial time, can limit large-scale model error while the model produces mesoscale output not resolved by the data. On a limited sample of cases they determined what assimilation method provides the most positive impact on model simulations. They found the best results for precipitation, planetary boundary layer (PBL) depth, surface-layer temperature, and wind fields were obtained by nudging toward 12-h rawinsonde wind, temperature, and moisture data above the model PBL.

Liu et al. (*13*) used the NCAR/Army Test and Evaluation Command (ATEC) real-time FDDA system, which was a MM5-based system used at the White Sands Missile Range. Their experiment showed that adding new data sources always reduced the error in the MM5, observations assimilated that are well distributed in time and space show the MM5 performs better than clustered observations, upper-air wind observations are most effective in driving the model to the "correct" solution, and surface observations are critical to the accuracy of the lower troposphere. Chang and Dumais (*14)* discovered that ingestion of ACARS data into a mesobeta simulation of a Texas large-scale convective event produced small amplitude and short duration temporal oscillations in the nudged fields that were the result of minor model adjustment processes.

Pattantyus (*7*) studied a dynamic case using the WRF over Yuma, AZ for a test using the Scan Eagle UAS in 2007. His emphasis was on precipitation forecasts; thus, he assimilated surface and upper-air data along with varying the radii of influence to see how it influenced the model precipitation fields in a dynamically-driven synoptic case. He found that smaller radii of influence produced more orographic precipitation. Varying the radii of influence also influenced the temperature and dew point field with the surface dew points showing the greatest improvement. In the upper levels, a larger radii of influence performed better than smaller radii. Additional work by Deng et al. (*15*) using the WRF with 4-km grid spacing and coarser grids, found improvements at all model levels and grid resolutions using FDDA. Szoke et al. (*16*) studied the influence of TAMDAR-U data on the 20-km Rapid Update Cycle model for numerous variables such as ceiling, visibility, and precipitation. They found a positive impact using TAMDAR-U input but noted that there were many cases where forecast differences were small or would improve one variable and not another. Recent work by Reen and Stauffer (*17*) has focused on improvement of nudging direct weather observations in the boundary layer (screen level, PBL, and even soil temperature), some of which are already in the WRF FDDA version we used for this study.

While there are many other studies done with FDDA there has been little work done with model horizontal spacing less than 4-km and 90-level vertical spacing. It is probably unreasonable to expect to run a 90-level model in a battlefield environment due to computational considerations, but this was still very useful work that adds detail about the WRF performance using just one additional upper-air data input to the model.

8. Conclusions

With an Army requirement to run the WRF at smaller time and space resolutions, many current data inputs, such as surface weather stations, upper-air radiosonde observations, and commercial ACARS observations are often inadequate since they still leave large gaps over many regions of the globe and/or times of day. The availability of such high spatial/temporal asynoptic weather observations is vital for high resolution numerical weather modeling systems and their associated atmospheric data assimilation systems. In a military operations application, surface observations and upper-air weather balloons are typically even sparser. To improve the input data sources, ARL combined with the PSL-TAAC and AirDat to design a system where TAMDAR-U was developed to fly on an UAS. Data collected by the TAMDAR-U were then ingested into the WRF model using FDDA. Four flight days were conducted, three of which were discussed in detail in this report. Afterwards, for each test day a double-nested configuration of WRF (version 3.2.1) was run centered near the test site location.

It was found in this study that the "method" works. ARL was able to gather data using TAMDAR-U instruments on an UAS and then assimilate these data into the WRF. This can be a very useful tool for the Army in data-sparse regions. The UAS is robust enough that it can fly at many levels and can fly for extended periods of time to provide continuous assimilation into the model. The fact that it can produce high frequency and multilevel direct observations of critical weather parameters (temperature, humidity, winds) was very advantageous for the FDDA observation nudging strategy used in this study at mesogamma scale WRF grid spacings.

Comparing the model output with and without the FDDA data, it was found that the temperature fields do not show much change between model runs, although this has not been studied or verified with any statistical methods. It appears that moisture fields show the most variation, while the wind speeds do increase slightly near the UAS location on the grid. The model corrections do propagate downwind, but these model adjustments can also be seen upwind, far removed from the location of the UAS and where the data were assimilated. Not only do these adjustments occur in space, they also occur in time. Several hours after the flight had ended there were still some slight differences noted in model fields. The model feedbacks were even noted to influence the rainfall amounts hours after the data had been ingested. The changes are seen in all directions and fields, including the vertical. However, as expected the strongest impacts were felt close to the time and space that data assimilation occurred. The results do show the impact of

FDDA can influence the model output. In this work, questions have not been answered about how much of an improvement was made in the model or even if there was improvement. Also, it is uncertain if these changes are significant. Future work by ARL will try and answer these questions with far more data and data sources ingested into the model. Studies will test as to how different variables are influenced, as well as better techniques for nudging coefficients and radii of influence. It is hoped that these studies can provide a better model solution that can improve weather forecasts in the battlefield at small scales.

9. References

1. National Center of Atmospheric Research. The Weather Research and Forecasting Model. http://wrf-model.org/index.php (accessed November 2011).
2. Physical Sciences Laboratory. NMSU Physical Science Laboratory Technical Analysis and Applications Center. http://www.psl.nmsu.edu/uav/ (accessed October 2011).
3. Physical Sciences Laboratory. NMSU Physical Science Laboratory Technical Analysis and Applications Center. http://www.psl.nmsu.edu/uav/sw-demo.php (accessed November 2011).
4. AirDat LLC. TAMDAR. http://www.airdat.com/tamdar/faq.php (accessed November 2011).
5. Aeronautics Defense Systems. http://www.aeronautics-sys.com/aerostar_tactical_auv (accessed November 2011).
6. National Aeronautics and Space Administration. First Results in on TAMDAR. http://aeronautics.nasa.gov/te06_tamdar.htm (accessed November 2011).
7. Pattantyus, A. Optimizing Strategies for an Observation-nudging-based Four-Dimensional Data Assimilation Forecast Approach with WRF-ARW. *Science and Engineering Apprenticeship Program*, Adelphi, MD, August 2011. (unpublished).
8. Xu, M., et al. Sensitivity study on nudging parameters for a mesoscale FDDA system, Preprint of the *15th Conference on Numerical Weather Prediction*, San Antonio, Texas, 2002; Paper 4B.4.
9. DCDBS. DCDBS table of contents. http://dcdbs.ssec.wisc.edu (accessed March 2012).
10. University of Wyoming. Department of Atmospheric Sciences. http://weather.uwyo.edu (accessed November 2011).
11. DCDBS. Satellite Inventory. http://dcdbs.ssec.wisc.edu/inventory (date March 2012).
12. Stauffer, D.R.; Seamon,N.L; Binkowski, F.S. Use of Four-Dimensional Data Assimilation in a Limited-Area Mesoscale Model Part II: Effects of Data Assimilation within the Planetary Boundary Layer. *Mon. Wea. Rev.* **1991**, *119*, 734−754.
13. Liu, Y., et al. Data Impact Experiments Using the NCAR/ATEC Real-Time FDDA and Forecast (RTFDDA) System, Preprint of The Battlespace Atmospheric and Cloud Impacts on Military Operations (BACIMO). *BACIMO*, Montery, CA, September 9−11, 2003; pp 1-12.
14. Chang, C.B.; Dumais,R.E. Mesoscale FDDA Experiments with WTM and ACARS Data. *The Open Atmospheric Science Journal* **2008**, *2*, 117−130.

15. Deng, A; Stauffer.D.R. On Improving 4-km Mesoscale Model Simulations. *J. Appl. Meteor* **2006**, *45***,** 361−381.

16. Szoke et al. Effect of TAMDAR Data on RUC Short-Term Forecasts of Aviation-Impact Fields For Celing, Visibility, Reflectivity, and Precipitation, *13th Conference on Aviation, Range, and Aerospace Meteorology*, New Orleans, LA, 2008; p. 64.

17. Reen, B.P.; Stauffer,D.R. Data Assimilation Strategies in the Planetary Boundary Layer. *Bound-Layer Meteor* **2010,** *137*, 237−269.

List of Symbols, Abbreviations, and Acronyms

ACARS	Aircraft Communications Addressing and Reporting System
AGL	above ground level
ARL	U.S. Army Research Laboratory
ARW	Advanced Research version of the WRF
ATEC	Army Test and Evaluation Command
COA	certificate of authorization
DCDBS	Digital Cadastral Data Bases
DSP	Digital Signal Processing
FDDA	Four-dimensional Data Assimilation
LRU	Las Cruces International Airport
MC	mission commander
MM	Mesoscale Model
MSL	mean sea level
NAM	North American Mesoscale
NAS	National Airspace System
NASA	National Aeronautics and Space Administration
NCAR	National Center of Atmospheric Research
PBL	planetary boundry layer
PSL	Physical Science Laboratory
RH	relative humidity
RRTM	Rapid Radiative Transfer Model
TAAC	Technical Analysis and Application Center
TAMDAR	Tropospheric Airborne Meta Data Processing
TAMDAR-U	Tropospheric Airborne Meta Data Processing-Unmanned Aircraft System
UAS	Unmanned Aircraft System
UTC	Coordinated Universal Time
WRF	Weather Research and Forecasting

No. of Copies	Organization
1 (PDF)	ADMNSTR DEFNS TECHL INFO CTR DTIC OCP 8725 JOHN J KINGMAN RD STE 0944 FT BELVOIR VA 22060-6218
3 HCs	US ARMY RSRCH LAB ATTN RDRL CIO LT TECHL PUB ATTN RDRL CIO LL TECHL LIB ATTN IMNE ALC HRR MAIL & RECORDS MGMT 2800 POWDER MILL ROAD ADELPHI MD 20783-1197
1 CD	ATMOSPHERIC PROPAGATION BRANCH SPAWARSYSCEN SAN DIEGO D858 49170 PROPAGATION PATH SAN DIEGO CA 92152-7385
1 CD	NCAR LIBRARY SERIALS NATL CTR FOR ATMOS RSCH PO BOX 3000 BOULDER CO 80307-3000
1 CD	HEADQUARTERS DEPT OF ARMY DAMI POB WEATHER TEAM 1000 ARMY PENTAGON ROOM 2E383 WASHINGTON DC 20310-1067
1 CD	HQ AFWA/DNX 106 PEACEKEEPER DR STE 2N3 OFFUTT AFB NE 68113-4039
1 CD	US ARMY CECRLCECRL GP ATTN DR DETSCH HANOVER NH 03755-1290
1 CD	USAF ROME LAB TECH CORRIDOR W STE 262 RL SUL 26 ELECTR PKWY BLD 106 GRIFFISS AFB ROME NY 13441-4514
1 CD	US ARMY OEC CSTE EFS PARK CENTER IV 4501 FORD AVE ALEXANDRIA VA 22302-1458
1 CD	US ARMY RESEARCH LAB RDRL CIE COMP & INFO SCI DIR WSMR NM 88002-5501
1 CD	WSMR TECH LIBRARY BR STEWS IM IT WSMR NM 88002
1 CD	NAVAL RESEARCH LABORATORY MARINE METEOROLOGY DIVISION 7 GRACE HOPPER AVENUE STOP 2 MONTEREY CA 93943-5502
1 CD	US ARMY RESEARCH LAB ATTN TERRY JAMESON RDRL CIE M WSMR NM 88002-5501
1 CD	US ARMY RESEARCH LAB ATTN STEPHEN KIRBY RDRL CIE M WSMR NM 88002-5501
3 HCs 4 CDs	US ARMY RESEARCH LAB ATTN J PASSNER RDRL CIE M WSMR NM 88002-5501

Total: 23 (1 PDF, 6 HCs, 16 CDs)

INTENTIONALLY LEFT BLANK.